Int J Earth Sci (Geol Rundsch) (2010) 99:813–832
DOI 10.1007/s00531-009-0425-5

ORIGINAL PAPER

U–Pb LA-SF-ICP-MS zircon geochronology of the Serbo-Macedonian Massif, Greece: palaeotectonic constraints for Gondwana-derived terranes in the Eastern Mediterranean

Guido Meinhold · Dimitrios Kostopoulos · Dirk Frei · Felix Himmerkus · Thomas Reischmann

Received: 6 May 2008 / Accepted: 5 February 2009 / Published online: 3 March 2009

Abstract The Pirgadikia Terrane in northern Greece forms tectonic inliers within the Vardar suture zone bordering the Serbo-Macedonian Massif to the southwest. It comprises Cadomian basement rocks of volcanic-arc origin and very mature quartz-rich metasedimentary rocks. U–Pb laser ablation sector-field inductively-coupled plasma mass spectrometry analyses of detrital zircons from the latter reveal a marked input from a Cadomian–Pan-African source with minor contribution from Mesoproterozoic, Palaeoproterozoic and Archaean sources. The metasedimentary rocks are correlated with Ordovician overlap sequences at the northern margin of Gondwana on the basis of their maturity and zircon age spectra. The Pirgadikia Terrane can be best interpreted as a peri-Gondwana terrane of Avalonian origin, which was situated close to the Cadomian terranes in the Late Neoproterozoic–Early Palaeozoic, very much like the Istanbul Terrane. The second unit investigated is the Vertiskos Terrane, which constitutes the major part of the Serbo-Macedonian Massif in Greece. It comprises predominantly igneous rocks of Silurian age and minor metasedimentary rocks of unknown age and provenance. U–Pb analyses of detrital zircons from a garnetiferous mica schist of the Vertiskos Terrane indicate derivation from 550 to 1,150 Ma-old source rocks with a major Cadomian peak. This, combined with minor input of >1,950 Ma-old zircons and the absence of ages between ca. 1.2 and 1.7 Ga suggests a NW Africa source. The protolith age of the garnetiferous mica schist is presumably Early Ordovician. One sample of garnet-bearing biotite gneiss, interpreted as meta-igneous rock, comprises predominantly subhedral zircons of igneous origin with late Middle Ordovician to Silurian ages. We suggest that the rock association of the Vertiskos Terrane is part of an ancient active-margin succession of the Hun superterrane, comparable to successions of the Austro- and Intra-Alpine Terranes. The new data of this study provide evidence of occurrences of Avalonia- and Armorica-derived terranes in the Eastern Mediterranean and moreover help to clarify palaeogeographic reconstructions for the peri-Gondwana realm in the Early Palaeozoic.

Keywords U–Pb zircon geochronology · Early Palaeozoic · North Gondwana · Serbo-Macedonian Massif

Electronic supplementary material The online version of this article (doi:10.1007/s00531-009-0425-5) contains supplementary material, which is available to authorized users.

G. Meinhold
Institut für Geowissenschaften, Johannes Gutenberg-Universität, Becherweg 21, 55099 Mainz, Germany

Present Address:
G. Meinhold (✉)
CASP, Department of Earth Sciences, University of Cambridge, 181a Huntingdon Road, Cambridge CB3 0DH, UK
e-mail: guido.meinhold@casp.cam.ac.uk

D. Kostopoulos
Department of Mineralogy and Petrology, National and Kapodistrian University of Athens, Panepistimioupoli Zographou, 15784 Athens, Greece

D. Frei
Geological Survey of Denmark and Greenland (GEUS), Øster Voldgade 10, 1350 Copenhagen K, Denmark

F. Himmerkus
Forschungszentrum Karlsruhe, Hermann-von-Helmholtz-Platz 1, 76344 Eggenstein-Leopoldshafen, Germany

T. Reischmann
Max-Planck-Institut für Chemie, Abt. Geochemie, Postfach 3060, 55020 Mainz, Germany

Introduction

Understanding ancient plate tectonic processes in space and time is strongly dependent on the accessibility and preservation of old crustal or oceanic fragments. Major tectonic and thermal events commonly lead to destruction and recycling of continental and oceanic crust, especially during orogenic processes at active continental margins. A prime example is the so-called Avalonian–Cadomian belt (Nance and Murphy 1994): its late Neoproterozoic to Early Palaeozoic evolution had an important bearing on the geological development of Europe (e.g. Neubauer 2002). The Avalonian–Cadomian belt was formed during late Neoproterozoic Andean-type subduction of the Prototethys Ocean under the northern margin of Gondwana (Nance and Murphy 1994; Stampfli and Borel 2002) and was subsequently dismembered in Cambrian to Silurian times with the diachronous opening of back-arc basins, giving birth to the Rheic Ocean and later on to the Palaeotethys Ocean (e.g. Stampfli and Borel 2002; Stampfli et al. 2002). It is widely agreed that the rifted fragments (Avalonian terranes, Hun superterrane including the Cadomian terranes) were transported northward to be accreted to the southern margin of Laurussia (e.g. Stampfli and Borel 2002; Stampfli et al. 2002; von Raumer et al. 2002, 2003). They became involved in the Late Palaeozoic Variscan orogeny and some of them were also overprinted by the Alpine–Himalayan orogeny in the Late Mesozoic to Cenozoic. The Alps, the Bohemian Massif, and the Carpathians are prominent areas in Central and Eastern Europe (Fig. 1) which comprise fragments of the Avalonian–Cadomian belt (e.g. Neubauer 2002). In the Eastern Mediterranean the relationships between different pre-Alpine crustal fragments are now masked by younger (Mesozoic to Cenozoic) complex structural and metamorphic events. This, together with the scarcity of biostratigraphic, geochronological and palaeomagnetic data, has given rise to equivocal palaeotectonic models and interpretations. Nonetheless, one of the main innovative topics in recent years has been the identification of Avalonia- and Armorica-derived terranes in the Eastern Mediterranean (e.g. Anders et al. 2006; Himmerkus et al. 2006a, 2007, 2008; Winchester et al. 2006; Yanev et al. 2006).

The Serbo-Macedonian Massif (SMM) of northern Greece (Figs. 1, 2 and 3) is a case in point. Upper Neoproterozoic and Silurian rocks of magmatic-arc origin have recently been discovered there (Himmerkus et al. 2006a, 2007, 2008), but their affiliation with surrounding basement units in Bulgaria and Turkey is still uncertain. In recent palaeotectonic reconstructions for the Cambrian–Ordovician (~490 Ma), for instance, the SMM is assigned to the Cadomian terranes close to Saxothuringia and Ligeria (Stampfli et al. 2002). Later, during the Carboniferous (~320 Ma) it is proposed to have become sandwiched between the Austro-Alpine unit to the southwest and the Sakarya terrane to the east (Stampfli et al. 2002). The data base for such reconstructions, however, is still lacking. No fossil data are available for the intercalated siliciclastic metasedimentary rocks of the SMM due to polyphase deformation and upper amphibolite-facies metamorphism (e.g. Kockel et al. 1971; Kilias et al. 1999). Their stratigraphic age is questionable and their provenance is unknown: they could have been derived from the Avalonian or the Armorican terranes, or from elsewhere. Hence, the age and origin of basement units of the Greece may well provide further insight into the configuration of North Gondwana-derived terranes in the Eastern Mediterranean.

In recent years, in situ U–Pb dating of detrital zircons by laser ablation inductively-coupled plasma mass spectrometry (LA-ICP-MS) has proven to be a powerful tool in sedimentary provenance studies (e.g. Fernández-Suárez et al. 2002; Košler et al. 2002; Murphy et al. 2004; Gerdes and Zeh 2006; Meinhold and Frei 2008). Here, we present for the first time high-spatial resolution U–Pb dating by laser ablation sector-field inductively-coupled plasma mass spectrometry (LA-SF-ICP-MS) of detrital and igneous zircon grains from basement rocks of the Serbo-Macedonian Massif and adjacent basement slivers to evaluate potential source regions and ancient major magmatic events.

The study of clastic sedimentary rocks is crucial for palaeotectonic reconstructions because they can provide information about rock lithologies in the source area which have often been destroyed and recycled during ancient plate tectonic processes. Furthermore, in the absence of fossil and other stratigraphic data, the youngest grain (e.g. zircon) in a sedimentary rock can indicate a maximum limit for the age of deposition (e.g. Fedo et al. 2003). The age and origin of pre-Alpine basement units in the Internal Hellenides has important implications for our in-depth understanding of the evolution of North Gondwana-derived terranes and consequently for an alternative plate-tectonic reconstruction for the Early Palaeozoic.

Geological setting

In the general view, the Serbo-Macedonian Massif in northern Greece is an elongated, structurally complicated basement complex between the relatively homogeneous basement complexes of the Pelagonian Zone to the west and the Rhodope Massif to the east. It extends north into western Bulgaria and eastern F.Y.R.O.M. The Vardar strike-slip zone marks its boundary with the Pelagonian Zone, while its border with the Rhodope Massif has long been a matter of debate.

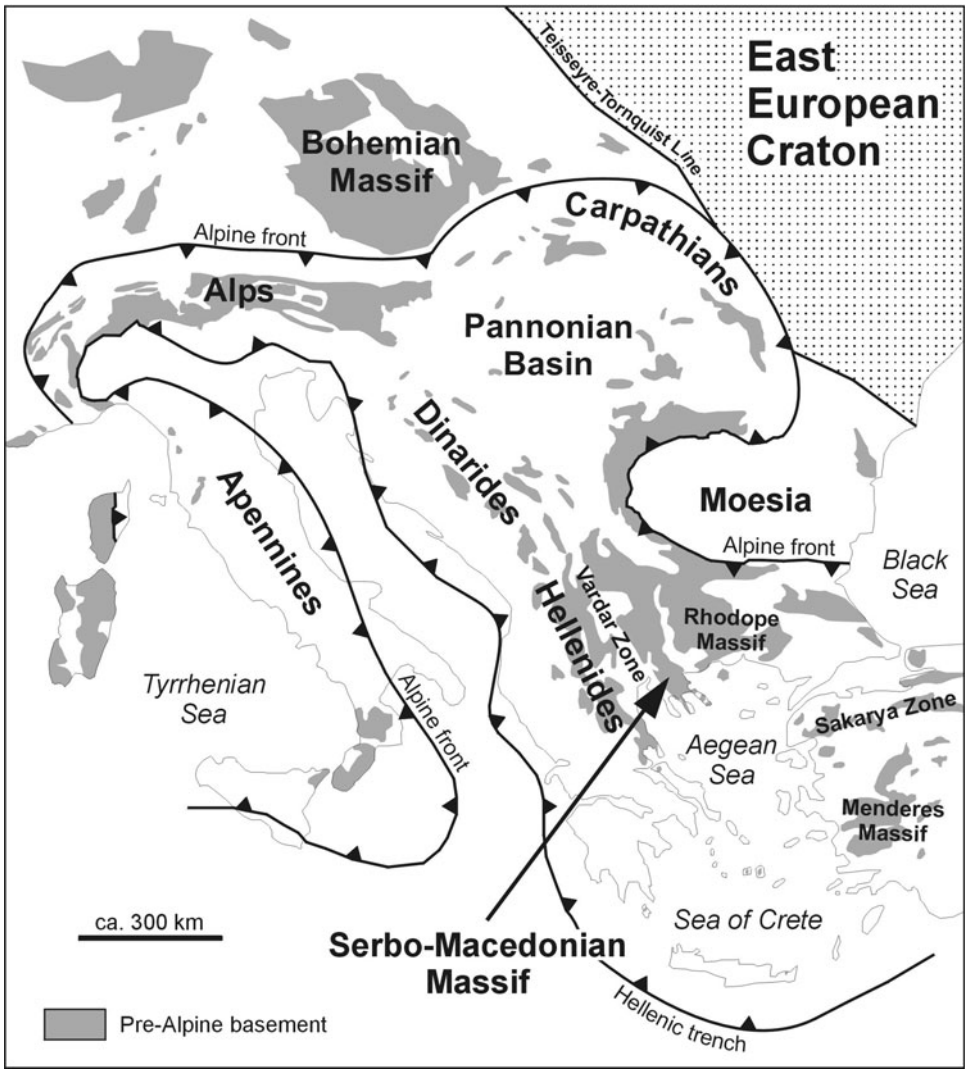

Fig. 1 Present-day location of the Serbo-Macedonian Massif within the Alpine–Mediterranean mountain belt (modified after Neubauer 2002)

Early workers suggested that the SMM was thrust over the Rhodope Massif along the Strimon River valley fault in the Tertiary (Kockel and Walther 1965; Kockel et al. 1971), but later this fault was reinterpreted as a large-scale, southwest-dipping, extensional detachment (e.g. Dinter and Royden 1993; Sokoutis et al. 1993; Kilias et al. 1999). Recently, however, Brun and Sokoutis (2007) have demonstrated that the Strimon fault is in fact a décollement within the Rhodope upper brittle crust that operated during Pliocene–Pleistocene times. Thus, the SMM does not structurally overlie the Rhodope Massif on the Strimon fault. According to Brun and Sokoutis (2007), the boundary between the SMM and the Rhodope Massif is represented by the WSW-dipping Kerdillion detachment that separates the Kerdillion Unit from the Vertiskos Terrane of the SMM (Fig. 4).

The Serbo-Macedonian Massif is mainly composed of amphibolite-facies schists and gneisses, locally migmatitic, amphibolites and marbles. Its subdivision and age have been a matter of controversy and lengthy discussions. It has conventionally been subdivided into two 'series', the underlying (older) Kerdillion Series to the east and the overlying (younger) Vertiskos Series to the west (Kockel et al. 1971, 1977). The rocks were thought to represent a Palaeozoic or older stable basement that was only superficially involved in the complex Mesozoic and Cenozoic evolution of the Hellenides (e.g. Aleksić et al. 1988; Kockel et al. 1971, 1977). Burg et al. (1995) demonstrated that the Vertiskos Series is a composite unit comprising a lower metaturbiditic and orthogneissic sequence, with few amphibolites and distinct marble layers, and an upper migmatitic para- and orthogneissic sequence, separated by a metaophiolite-bearing mylonite zone. Ricou et al. (1998) suggested that the Serbo-Macedonian Massif represents the western extension of thrust units belonging to the Rhodope Massif, the latter commonly interpreted as a nappe complex characterised by south to southwestward stacking and associated with both coeval and subsequent extension in an Alpine active-margin setting (Burg et al. 1996).

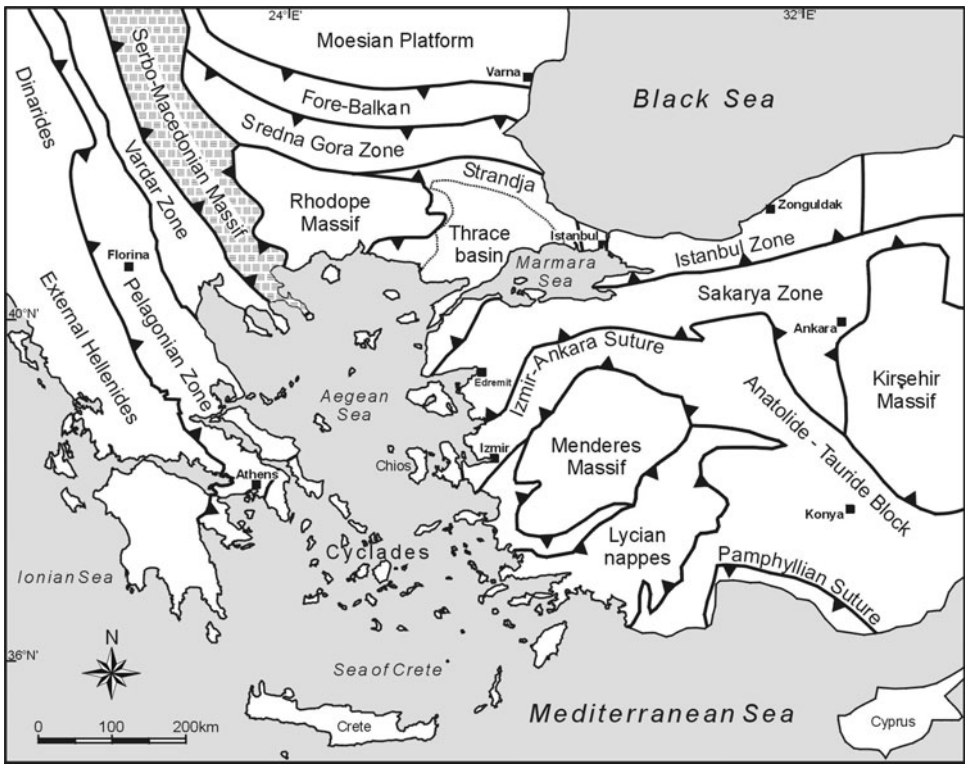

Fig. 2 Simplified tectonic map of the Eastern Mediterranean showing the major geotectonic units and the bounding sutures (modified from Meinhold et al. 2008)

Geochronological and geochemical studies carried out over the last few years have provided us with new insights regarding the Serbo-Macedonian Massif (Himmerkus et al. 2006a, b, 2007, 2008, 2009). Its western and central parts are formed by the Vertiskos Terrane. This unit consists dominantly of very coarse-grained augen gneisses of granitic composition which originated in a magmatic-arc environment (Himmerkus et al. 2006a, 2008); lesser amounts of eclogites, amphibolites, marbles, mica schists and paragneisses also occur. Pb–Pb and U–Pb zircon geochronology has shown a Silurian age for the augen gneisses (Himmerkus et al. 2006a, 2008). The basement rocks of the Vertiskos Terrane were intruded by Triassic (ca. 222–241 Ma) A-type granitoids (Arnea granitic suite) in a within-plate rift setting together with a number of mafic intrusives, interpreted as less evolved magmas (Himmerkus et al. 2009). The rocks of the Vertiskos Terrane underwent amphibolite-facies metamorphism and a retrograde greenschist-facies overprint (e.g. Dixon and Dimitriadis 1984; Kilias et al. 1999). Because all contacts are tectonic, there is no clear relationship with the surrounding country rocks.

The eastern and southeastern part of the Serbo-Macedonian Massif is formed by the Kerdillion Unit. This unit is very homogeneous, consisting of strongly deformed biotite-gneisses of igneous origin, which are intruded by a plethora of leucocratic dykes. Carboniferous–Permian, Late Jurassic and Early Tertiary magmatic events have been identified by zircon geochronology (Himmerkus et al. 2006b, 2007). Thus, the Kerdillion Unit can be seen as the western promontory of the adjacent Rhodope Massif where similar intrusion ages and rock types have also been found (Turpaud and Reischmann 2005; Turpaud 2006). The boundary between the Kerdillion Unit and the Vertiskos Terrane is interpreted as a suture (e.g. Şengör et al. 1984; Himmerkus et al. 2006a), consisting of a mélange of marble, amphibolite and metagabbro bodies, several tens of metres thick, floating in a metasedimentary succession. The mafic–ultramafic rocks have generally been assigned to the so-called Therma–Volvi–Gomati (TVG) Complex (e.g. Dixon and Dimitriadis 1984) and commonly been interpreted as either a remnant of the Palaeotethys Ocean that closed in the Early Jurassic (Şengör et al. 1984) or, in contradiction, as a rift-related intrusive complex of Mesozoic age (Dixon and Dimitriadis 1984). In comparison, Brun and Sokoutis (2007) suggest that the boundary between the Kerdillion Unit and the Vertiskos Terrane is represented by the WSW-dipping Kerdillion detachment (Fig. 4).

Recently, Neoproterozoic basement rocks have been identified as tectonic inliers within the Circum-Rhodope Belt (part of the Vardar Zone sensu Jacobshagen 1986) bordering the Serbo-Macedonian Massif to the southwest (Himmerkus et al. 2006a). The main outcrops occur near the villages of Pirgadikia and Taxiarchis. Himmerkus et al. (2006a) proposed a Pirgadikia Terrane based on

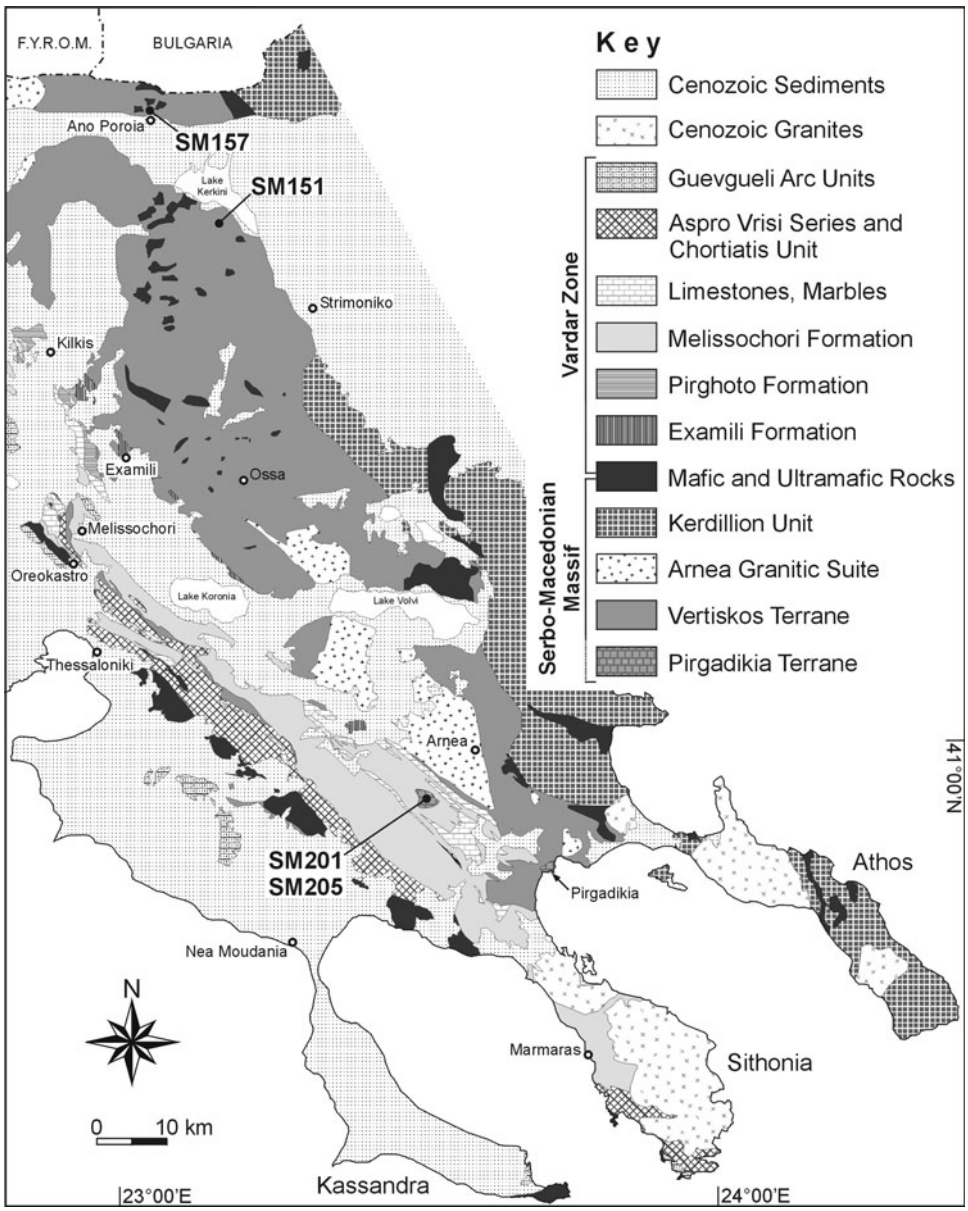

Fig. 3 Geological map of the Serbo-Macedonian Massif and the bordering Vardar Zone (modified from Kockel and Mollat 1977; IGME 1983) showing the sampling locations used for zircon geochronology. The occurrences of the Kerdillion Unit are after Himmerkus et al. (2006a). In general, the Serbo-Macedonian Massif sensu lato includes the Kerdillion Unit, which itself, however, can be seen as the western promontory of the adjacent Rhodope Massif, based on new field and geochronological data (Himmerkus et al. 2006b, 2007)

lithological, geochronological and structural features that differ strongly from those of units belonging to the Serbo-Macedonian Massif and the adjacent basement rocks of the Pelagonian Zone and the Rhodope Massif. The Pirgadikia Terrane near Pirgadikia village consists of mylonitic orthogneisses. Their geochemistry and zircon ages point to volcanic-arc magmatism during late Precambrian times (Himmerkus et al. 2006a).

In the course of this study, the area near Taxiarchis village was revisited. The basement rocks there are of sedimentary origin, consisting mainly of fine- to coarse-grained, well sorted, and light coloured to greenish-grey metaquartzites intercalated with greenish grey metasiltstones; conglomerate horizons up to one metre thick occur sporadically. The metaquartzites in places show a strong mylonitic fabric. The conglomerates are predominantly composed of milky-white quartz pebbles embedded in a coarse-grained quartzose matrix. The width of the pebbles ranges from a few mm to 1.5 cm. Since no fossils have yet been discovered, the age of the metasedimentary succession is open to question. Previous single-zircon Pb–Pb age determinations for a mylonitic metaquartzite range between ca. 530 and 590 Ma, probably indicating proximity to a Cadomian basement (Himmerkus et al. 2006a). The circa 530 Ma age can be considered as representing the youngest detrital input thus giving a maximum age of deposition for the metasedimentary rocks of the Pirgadikia Terrane.

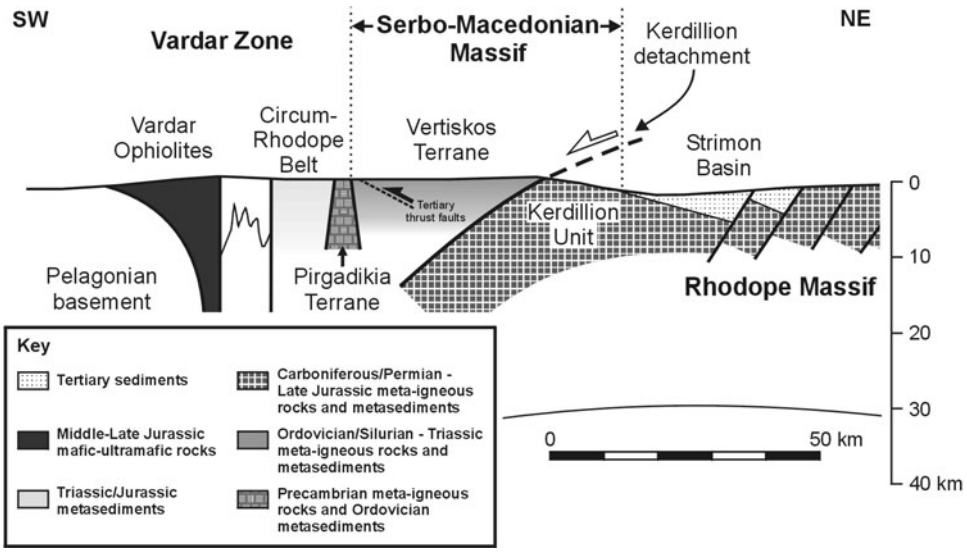

Fig. 4 Synthetic cross section illustrating the tectonic relationships between the Vertiskos and Pirgadikia terranes and neighbouring units (modified after Brun and Sokoutis 2007, and results of the Mainz Research Group)

Analytical methods

Major and trace elements of whole-rock samples were analysed by X-ray fluorescence (XRF) spectrometry on fused glass discs and pressed powder pellets respectively, using a Philips MagiX Pro X-ray spectrometer at the University of Mainz, following procedures outlined in Meinhold et al. (2007). Rare-earth elements (REE), Hf, Ta, Th and U of selected samples were analysed on fused discs by LA-ICP-MS using an Agilent 7500ce equipped with a Merchantek NewWave 213 nm Nd-YAG laser at the University of Mainz, following procedures described in Nehring et al. (2008).

For U–Pb geochronology zircons were separated from the bulk samples using standard techniques [hydraulic press, rotary mill, Wilfley table, Frantz isodynamic magnetic separator and heavy liquids (methylene iodide)]. Final purification was carried out by hand-picking under a binocular microscope. Zircon grains were set in epoxy resin mounts, sectioned and polished to approximately half their original thickness. Prior to the analyses, cathodoluminescence (CL) images were obtained for all grains using a JEOL JXA 8900 RL instrument at the University of Mainz equipped with a CL detector in order to study their internal structure and to target specific areas within them, e.g. growth structures and inherited cores.

The U–Pb isotopic analyses of individual zircon grains were performed using a Thermo-Finnigan Element II sector-field ICPMS system coupled to a Merchantek/NewWave 213 nm Nd-YAG laser system at the Geological Survey of Denmark and Greenland (GEUS), Copenhagen, Denmark. The zircon mounts were rigorously cleaned in an ultrasonic bath before introducing them into the sample cell to remove surface lead contamination. The method applied essentially followed that described by Frei and Gerdes (2008). The nominal pulse width of the laser was 5 ns with a pulse-to-pulse stability of 2% RSD. The laser was operated at a repetition rate of 10 Hz and a nominal energy output of 40%, corresponding to a laser energy of $\sim$0.006 mJ and a laser fluency of $\sim$0.8 J cm^{-2}. All data were acquired with single-spot analyses on individual zircon grains using a 30 μm spot size. Samples and standards were held in a low-volume ablation cell specially developed for U–Pb-dating (Horstwood et al. 2003). Helium gas was used to flush the sample cell and was mixed downstream with the Ar sample gas of the mass-spectrometer. The washout time for this configuration is <15 s. The total acquisition time for each analysis was 60 s with the first 30 s used to measure the gas blank. The instrument was tuned to give large, stable signals for the ^{206}Pb and ^{238}U peaks, low background count rates (typically around 150 counts per second for ^{207}Pb) and low oxide production

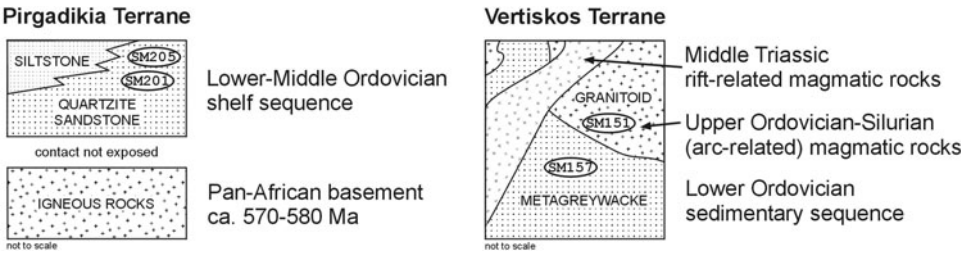

Fig. 5 Schematic tectonostratigraphic columns for the Pirgadikia and Vertiskos Terranes (see text for references). The stratigraphic positions of samples used for U–Pb zircon geochronology are indicated

Table 1 Sample list

Sample	Rock type	Locality	Latitude	Longitude
Pirgadikia Terrane				
SM201	Metaquartzite	NE′ Taxiarchis	40°26′00.7″	23°30′58.1″
SM202	Metasiltstone	NE′ Taxiarchis	40°26′04.0″	23°31′02.3″
SM204	Metaquartzite	NE′ Taxiarchis	40°25′45.6″	23°30′57.6″
SM205	Metaquartzite	NE′ Taxiarchis	40°25′39.1″	23°30′51.8″
SM208	Metaquartzite	E′ Taxiarchis	40°25′36.1″	23°30′44.4″
SM209	Metaquartzite	E′ Taxiarchis	40°25′36.1″	23°30′44.4″
SM250	Metasiltstone	E′ Taxiarchis	40°25′25.6″	23°30′39.3″
SM251	Metaquartzite	E′ Taxiarchis	40°25′36.1″	23°30′44.5″
SM252	Metaquartzite	NE′ Taxiarchis	40°25′58.3″	23°30′58.2″
Vertiskos Terrane				
SM151	Garnet-bearing biotite gneiss	W′ Agh. Iraklio	41°07′44.4″	23°12′13.7″
SM157	Garnetiferous mica schist	N′ Ano Poroia	41°17′27.3″	23°02′00.0″

rates ($^{238}U^{16}O/^{238}U$ generally below <0.2%). All measurements were performed in low resolution mode using electrostatic scanning (E-scan) with the magnetic field resting at mass ^{202}Hg. The following masses were measured: ^{202}Hg, $^{204}(Pb + Hg)$, ^{206}Pb, ^{207}Pb, ^{208}Pb, ^{232}Th, ^{235}U, and ^{238}U. All data were acquired on four samples per peak with a sampling and settling time of 1 ms for each isotope. Mass ^{202}Hg was measured to monitor the ^{204}Hg interference on ^{204}Pb (using a $^{202}Hg/^{204}Hg$-ratio of 4.36). Only if the net intensities for mass ^{204}Pb, corrected for ^{204}Hg, were significantly above the limit of detection a correction for common Pb was applied (see Frei and Gerdes 2008). The laser-induced elemental fractionation and instrumental mass biases on measured isotopic ratios were corrected by matrix-matched external standardisation using the GJ-1 zircon standard (Jackson et al. 2004). Samples were analysed in sequences with three standards analysed initially, followed by ten samples, then three standards, followed once again by ten samples, and so on. Raw data were processed off-line in an in-house Excel® spreadsheet program. Long-term precision (2σ) of the method based on 402 individual analyses of the Plešovice zircon standard (Sláma et al. 2008) is 2.2, 3.1 and 2.1% for the $^{206}Pb/^{238}U$, $^{207}Pb/^{235}U$ and $^{207}Pb/^{206}Pb$ ratios respectively (Frei and Gerdes 2008).

For the interpretation of the zircon data, analyses with 95–105% concordance [calculated from 100 × ($^{206}Pb/^{238}U$ age)/($^{207}Pb/^{235}U$ age)] are considered to be concordant. Analyses with a discordance >10% were rejected and consequently not considered for data interpretation. Such high discordance arises when the laser penetrates domains with distinct Pb/U ratios (Janoušek et al. 2006), the epoxy resin, mineral inclusions and/or cracks in zircon, and/or zircon zones affected by radiogenic Pb loss. The latter is a common phenomenon and mostly attributed to metamictisation and later recrystallisation during which Pb is removed from the zircon crystals (e.g. Williams 1992; Mezger and Krogstad 1997). Unless stated otherwise, $^{206}Pb/^{238}U$ ages are used for zircon grains <1.2 Ga whereas older grains are quoted using their $^{207}Pb/^{206}Pb$ ages. This is because the $^{207}Pb/^{206}Pb$ ages become increasingly imprecise below <1.2 Ga due to small amounts of ^{207}Pb. The $^{207}Pb/^{206}Pb$ ages are generally considered as minimum ages due to the effect of possible Pb loss. Concordia diagrams and probability density distribution plots were produced using the programs Isoplot/Ex (Ludwig 2003) and AgeDisplay (Sircombe 2004) respectively. Unless stated otherwise, ages reported in the text are given at the 2-sigma level. The geological time scale (GTS) of Gradstein et al. (2004) was used as stratigraphic reference for data interpretation.

Sample description and geochemistry

To constrain the age and provenance of basement rocks from the Serbo-Macedonian Massif and adjacent basement slivers, we have collected two metaquartzites from the Pirgadikia Terrane and one garnetiferous mica schist and one garnet-bearing biotite gneiss from the Vertiskos Terrane for zircon geochronology. Sample localities are shown in Figs. 3 and 5. These samples as well as additional ones from the Pirgadikia Terrane were also analysed for their whole-rock major- and trace-element content. Lithologies and localities (including geographic coordinates) are shown in Table 1, the whole-rock and mineral chemical data are given in Tables 2, 3, respectively, and the isotopic data of 226 analyses on 219 single zircon grains referred to in this paper are listed in Table 4 of supplementary material.

Table 2 XRF whole-rock geochemical data of investigated rocks

Unit	Pirgadikia Terrane									Vertiskos Terrane	
Sample no.	SM201	SM202	SM204	SM205	SM208	SM209	SM250	SM251	SM252	SM151	SM157
Rock type	metaquartzite	metasiltstone	metaquartzite	metaquartzite	metaquartzite	metaquartzite	metasiltstone	metaquartzite	metaquartzite	garnet-bearing biotite gneiss	garnetiferous mica schist
SiO_2 (wt%)	84.28	63.42	94.73	96.54	85.18	92.55	59.74	86.22	72.91	67.41	69.29
TiO_2	0.60	1.08	0.06	0.27	0.47	0.78	1.23	0.26	0.64	0.59	0.72
Al_2O_3	5.50	15.91	1.68	1.56	5.82	1.89	17.86	4.78	10.73	15.57	13.87
Fe_2O_3	4.46	7.70	1.21	0.61	3.57	2.49	7.84	4.50	6.70	4.50	4.94
MnO	0.07	0.09	0.01	0.00	0.05	0.02	0.11	0.05	0.07	0.06	0.07
MgO	1.08	2.47	0.18	0.00	0.88	0.35	2.25	0.91	1.64	1.36	2.12
CaO	0.18	0.76	0.04	0.02	0.26	0.20	0.38	0.09	0.38	3.27	1.36
Na_2O	1.06	1.68	0.38	BD	1.34	0.26	0.77	0.26	1.28	3.24	2.39
K_2O	0.45	3.23	0.12	0.49	0.56	0.21	4.50	0.59	1.76	2.90	3.33
P_2O_5	0.03	0.09	0.01	0.00	0.05	0.11	0.07	0.06	0.06	0.17	0.21
LOI	1.65	3.83	0.73	0.46	1.47	0.71	3.62	1.82	3.47	0.79	1.41
Total	99.37	100.26	99.14	99.95	99.65	99.58	98.37	99.52	99.64	99.84	99.70
Sc (ppm)	7	21	1	BD	6	4	28	7	17	10	11
V	64	129	12	15	49	44	150	53	89	60	86
Cr	46	96	7	12	45	35	114	27	77	27	68
Co	8	14	2	BD	8	2	13	8	10	7	14
Ni	13	35	2	1	11	7	34	14	26	11	28
Cu	5	5	4	20	5	2	20	10	6	10	21
Zn	40	89	16	7	36	19	93	40	76	66	80
Ga	6	19	2	2	6	3	20	6	12	20	17
Rb	16	99	5	17	21	8	140	21	60	92	119
Sr	31	48	10	9	47	17	98	15	68	236	170
Y	17	31	10	9	19	38	24	26	35	32	28
Zr	221	237	42	136	167	177	348	90	156	177	188
Nb	9	25	2	5	7	9	20	5	12	13	13
Ba	144	703	67	133	223	70	765	160	418	850	755
Hf	*5.79*	ND	ND	ND	ND	ND	ND	*2.16*	ND	*5.23*	*5.42*
Ta	*0.47*	ND	ND	ND	ND	ND	ND	*0.23*	ND	*0.97*	*1.15*
Th	*6.17*	7.6	1.0	0.4	2.6	2.3	13.2	*3.18*	4.9	*15.13*	*11.62*
U	*0.96*	3.5	1.5	0.8	1.3	1.2	3.6	*0.60*	0.5	*2.47*	*3.00*
La	*18.02*	24	9	10	25	10	24	*13.69*	28	*44.12*	*31.24*
Ce	*39.95*	40	20	6	42	20	42	*14.71*	49	*87.19*	*66.66*
Pr	*4.47*	6	2	2	3	3	10	*4.00*	6	*10.22*	*7.63*

Table 2 continued

Unit	Pirgadikia Terrane								Vertiskos Terrane	
Sample no.	SM201	SM202	SM204	SM205	SM208	SM209	SM250	SM251	SM252	SM151	SM157
Rock type	metaquartzite	metasiltstone	metaquartzite	metaquartzite	metaquartzite	metaquartzite	metasiltstone	metaquartzite	metaquartzite	garnet-bearing biotite gneiss	garnetiferous mica schist
Nd	*17.33*	22	10	7	22	10	23	*16.05*	27	*40.52*	*29.80*
Sm	*3.35*	4	4	3	6	4	4	*3.95*	7	*7.96*	*6.00*
Eu	*0.69*	ND	ND	ND	ND	ND	ND	*0.86*	ND	*1.28*	*1.24*
Gd	*2.86*	ND	ND	ND	ND	ND	ND	*4.20*	ND	*7.11*	*5.35*
Tb	*0.43*	ND	ND	ND	ND	ND	ND	*0.59*	ND	*1.02*	*0.82*
Dy	*2.59*	ND	ND	ND	ND	ND	ND	*4.03*	ND	*6.26*	*5.26*
Ho	*0.51*	ND	ND	ND	ND	ND	ND	*0.78*	ND	*1.20*	*1.05*
Er	*1.43*	ND	ND	ND	ND	ND	ND	*2.19*	ND	*3.38*	*2.89*
Tm	*0.23*	ND	ND	ND	ND	ND	ND	*0.29*	ND	*0.50*	*0.43*
Yb	*1.69*	ND	ND	ND	ND	ND	ND	*1.77*	ND	*3.14*	*2.80*
Lu	*0.24*	ND	ND	ND	ND	ND	ND	*0.24*	ND	*0.47*	*0.46*

BD below detection limit; *ND* not determined. Total iron expressed as Fe_2O_3. Analyses performed with ICP-MS are shown in italics

Table 3 Representative garnet chemistry of sample SM151

Sample	SM151-Gt1	SM151-Gt2	SM151-Gt3	SM151-Gt4
SiO_2 (wt%)	38.31	37.78	38.16	38.33
TiO_2	0.03	0.10	0.05	0.06
Al_2O_3	21.62	21.68	21.61	21.69
FeO_T	23.80	20.95	23.22	22.36
MnO	1.61	4.66	2.28	3.24
MgO	1.47	0.87	1.25	1.24
CaO	13.72	14.42	13.93	13.95
Cr_2O_3	0.06	0.02	0.06	0.05
Total	100.62	100.48	100.55	100.91
Cations on the basis of 12 oxygens				
Si	3.004	2.974	2.998	3.000
Ti	0.002	0.006	0.003	0.003
Al	1.998	2.011	2.001	2.001
Fe	1.561	1.379	1.525	1.464
Mn	0.107	0.311	0.152	0.215
Mg	0.172	0.102	0.146	0.145
Ca	1.153	1.216	1.172	1.170
Cr	0.004	0.001	0.003	0.003
End member percentages				
Alm	52	46	51	49
Gro	39	40	39	39
Prp	6	3	5	5
Sp	4	10	5	7

Mineral analyses were carried out on a polished thin section using a Jeol JXA 8900 RL electron microprobe at the University of Mainz, equipped with 5 wavelength-dispersive spectrometers, operated at an acceleration voltage of 20 kV and a beam current of 20 nA, with a beam diameter of 2 μm. Natural and synthetic materials were used as standards. The PRZ procedure was applied to calculate concentration units. Cations were calculated stoichiometrically based on 12 oxygens per formula unit

Pirgadikia Terrane

Sample SM201 was collected from a metaquartzite succession cropping out along a minor road northeast of Taxiarchis village (40°26′00.7″N, 23°30′58.1″E; Fig. 3); sample SM205 comes from a small metaquartzite outcrop along a new road southwest of Taxiarchis (40°25′39.1″N, 23°30′51.8″E; Fig. 3). The samples are almost feldspar-free quartz arenites with chlorite and accessory zircon, apatite and opaque minerals (Fe-oxides). All quartz grains are single crystals with almost no undulose extinction. Some larger grains show undulose extinction and subgrain formation. The quartz grain boundaries are almost straight, only a few are sutured. In general, the textures indicate that the quartz grains underwent dynamic recrystallisation (Passchier and Trouw 2005), probably at upper greenschist-facies conditions. The zircons in both samples are predominantly well-rounded to rounded, only a few are

subhedral. The length of single zircon crystals varies between 50 and 220 μm in sample SM201 and between 80 and 320 μm in sample SM205. Their colour ranges from pink and yellowish to whitish.

Geochemically, the metasedimentary rocks from the Pirgadikia Terrane are very mature sediments falling into two distinct groups: a medium- to high-SiO_2, high-Al_2O_3 group (SiO_2: 60–73 wt%, $Na_2O + K_2O + CaO$: 3.4–5.7 wt%, Al_2O_3: 11–18 wt%) that comprises metapelites and a very high-SiO_2, low-Al_2O_3 group (SiO_2: 84–96 wt%, $Na_2O + K_2O + CaO$: < 2.2 wt%, Al_2O_3: ≤ 6 wt%) that comprises metapsammites (Fig. 6a). According to the classification scheme of Herron (1988), the metapelites are shales and the metapsammites are iron-bearing sandstones and quartz arenites. Compared to average upper continental crust the low-Al_2O_3 group samples show a strong depletion in Rb, Ba, K, Sr and P, whereas those of the high-Al_2O_3 group have an almost flat profile with a characteristic depletion in Sr and P (Fig. 6a). Chondrite-normalised rare-earth element (REE) patterns of two metaquartzite samples used for zircon geochronology (Fig. 6b) show light rare-earth element (LREE) enriched and flat to slightly depleted heavy rare-earth element (HREE) patterns with a negative Eu anomaly (Eu/Eu* $\sim$0.68 for SM201 and $\sim$0.64 for SM206). The negative Ce anomaly of sample SM205 might be a result of quartz dilution since this sample has the highest SiO_2 content but very low trace- and rare-earth element concentrations.

Vertiskos Terrane

Sample SM157 was collected from an outcrop north of Ano Poroia village ca. 4 km south of the border with Bulgaria (41°17′27.3″N, 23°02′00.0″E; Fig. 3), where garnetiferous mica schists are exposed. Augen gneisses with large feldspar porphyroblasts measuring up to 5 cm across and migmatitic gneisses occur nearby. The main fabric in the area is an almost flat-lying foliation. Sample SM157 contains quartz, biotite, white mica, plagioclase, and minor garnet. The main accessory minerals are zircon, rutile and opaque minerals. The zircon crystals are predominantly subhedral to rounded, yellowish to colourless and clear. The length of single zircon crystals varies between 60 and 360 μm. According to the classification scheme of Herron (1988), the protolith of the garnetiferous mica schist is a wacke (i.e. greywacke). The SiO_2 content of $\sim$70 wt%, $Na_2O + K_2O + CaO$ content of $\sim$7 wt% and relatively high Al_2O_3 content of $\sim$14 wt% suggest a peraluminous composition. When normalised to average upper-continental crust this rock shows an almost flat multi-element profile with a minor depletion in Sr (Fig. 6a). The chondrite-normalised REE pattern (Fig. 6b) shows a strong LREE enrichment and an almost flat HREE region with a negative Eu anomaly (Eu/Eu* $\sim$0.67).

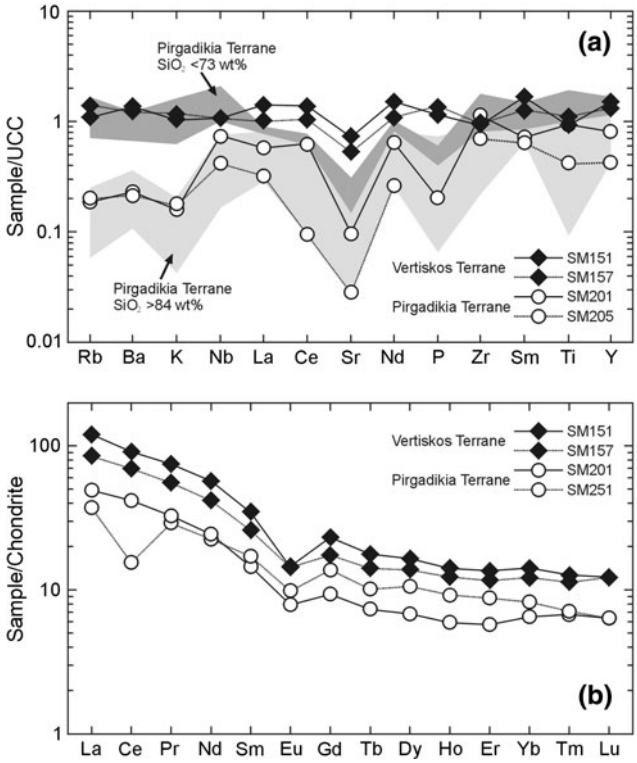

Fig. 6 **a** Multi-element diagram normalised to upper continental crust (UCC) composition of samples used for zircon geochronology. Normalising values are from Rudnick and Gao (2003). For comparison purposes, the remaining metasedimentary samples of the Pirgadikia Terrane are shown as *light* and *dark greyish* fields, respectively, according to their SiO_2 concentrations. **b** Chondrite-normalised rare-earth element (REE) diagram of selected samples. Normalising values are from Taylor and McLennan (1985)

Sample SM151 was collected from a small outcrop along a stream south of Lake Kerkini (41°07′44.4″N, 23°12′13.7″E; Fig. 3), in which garnet-bearing biotite gneiss, interpreted here as meta-igneous rock, is exposed. Amphibolites and tourmaline-bearing pegmatites crop out in the vicinity. The main fabric here is an almost flat-lying foliation accompanied by a strong ENE-trending biotite mineral lineation. Sample SM151 contains quartz, plagioclase, biotite, white mica, K-feldspar, garnet, zoisite and epidote. The garnet crystals are almandine and grossular rich (Alm $\sim$50 mol%, Grs $\sim$40 mol%). Accessory minerals are zircon, rutile and opaque minerals. The long, prismatic zircon crystals are euhedral with rounded edges to subhedral, clear colourless. The length of single zircon crystals varies between 100 and 300 μm. The chemical signature of the garnet-bearing biotite gneiss (SiO_2: $\sim$67 wt%, $Na_2O + K_2O + CaO$: $\sim$9 wt%, Al_2O_3: $\sim$15 wt%) suggests a calcalkaline, peraluminous and granodioritic composition with I-type affinities. Geochemical discrimination diagrams for granitoid rocks

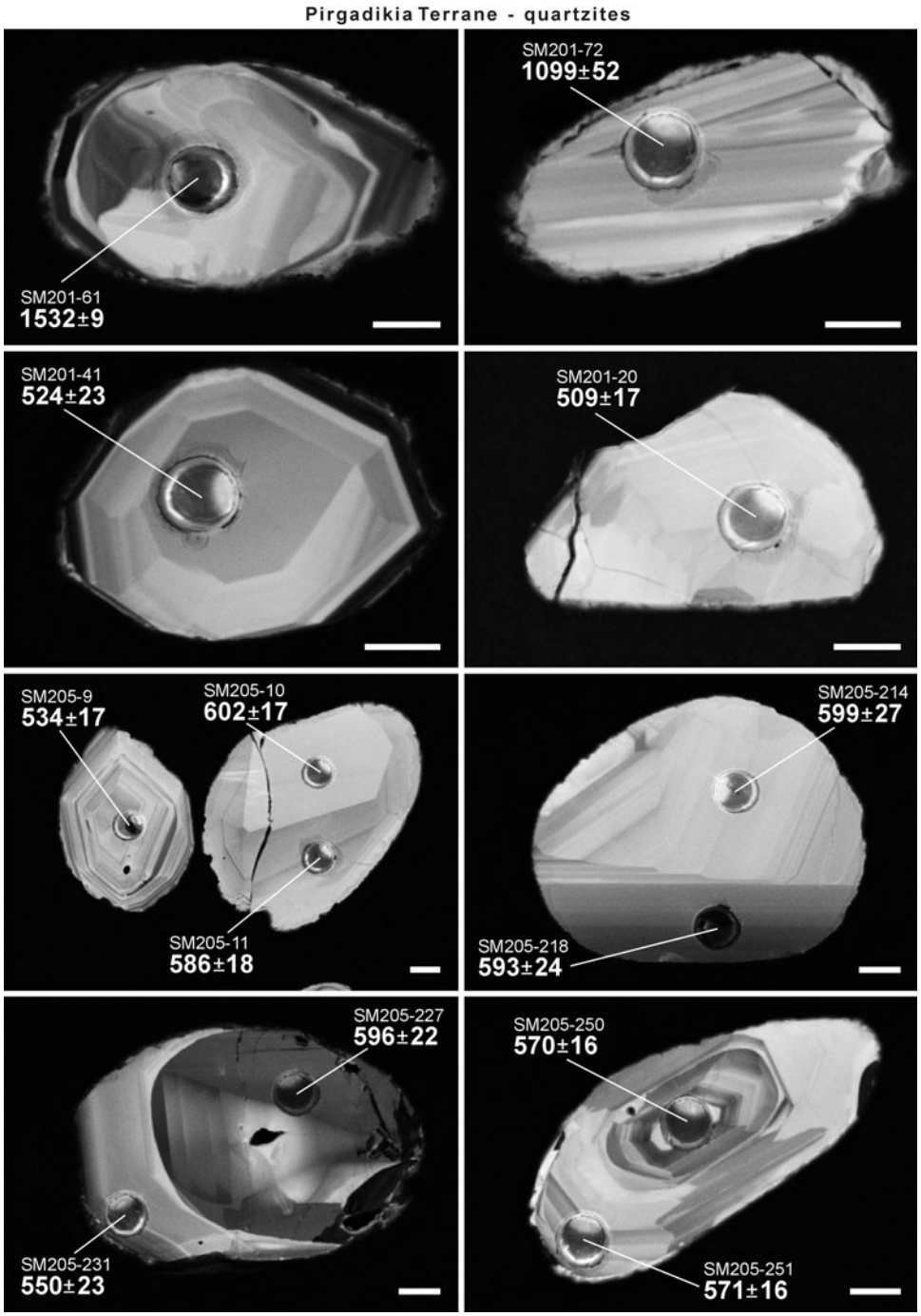

Fig. 7 CL images of representative zircon grains from analysed samples SM201 and SM205 of the Pirgadikia Terrane with location of the LA-SF-ICP-MS analysis spot and corresponding $^{206}U/^{238}Pb$ age ($\pm 2\sigma$) for grains <1.2 Ga and $^{207}Pb/^{206}Pb$ age ($\pm 2\sigma$) for grains >1.2 Ga, respectively. *Letter*, *number* code above the ages: sample-spot. The *scale bar* represents 30 μm in all images

(e.g. Yb vs. Ta, [Y + Nb] vs. Rb; see Pearce et al. 1984) reveal a volcanic-arc signature with affinities with within-plate granites. The multi-element pattern of sample SM151 is almost flat with a minor depletion of Sr, compared to average upper-continental crust composition (Fig. 6a). The chondrite-normalised REE pattern (Fig. 6b) shows a strong LREE enrichment and almost flat HREE region with a well-developed negative Eu anomaly (Eu/Eu* ~0.52).

Geochronological results

Pirgadikia Terrane

Most analysed zircons from metaquartzites of the Pirgadikia Terrane have clear oscillatory zonation patterns in CL images and appear to be magmatic in origin; few exhibit no zoning or patchy zoning (Fig. 7). Inherited cores are present to a minor degree in sample SM201 and are

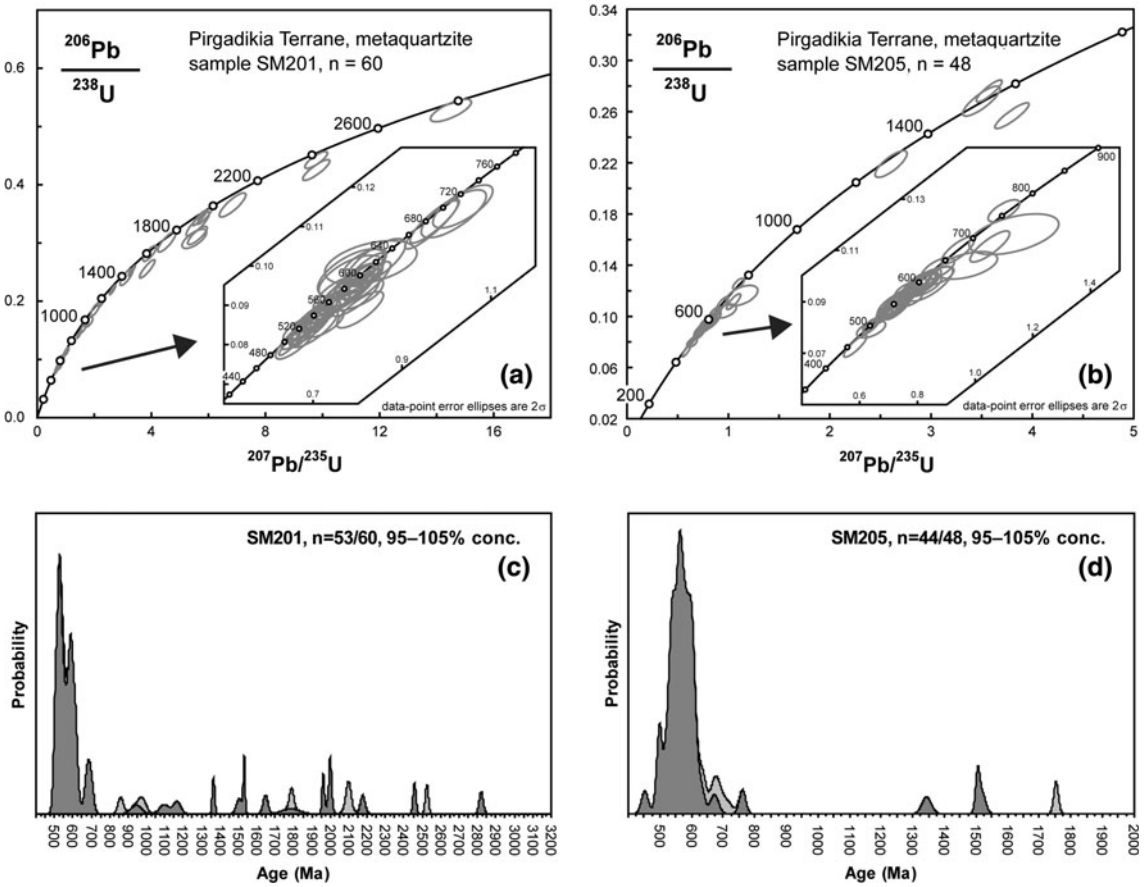

Fig. 8 Concordia diagrams (*upper*) and probability density distribution plots (*lower*) for the set of U–Pb analytical zircon data from samples SM201 (**a**, **c**) and SM205 (**b**, **d**). Error ellipses in concordia plots represent 2σ uncertainties. 1.2 Ga limit is used to switch between $^{206}Pb/^{238}U$ and $^{207}Pb/^{206}Pb$ ages for the probability plot. Probability density distribution plots: *dark grey* shaded zircon ages with 95–105% concordance, *light grey* shaded zircon ages with >5% discordance (see text for explanation). *n* Number of analyses

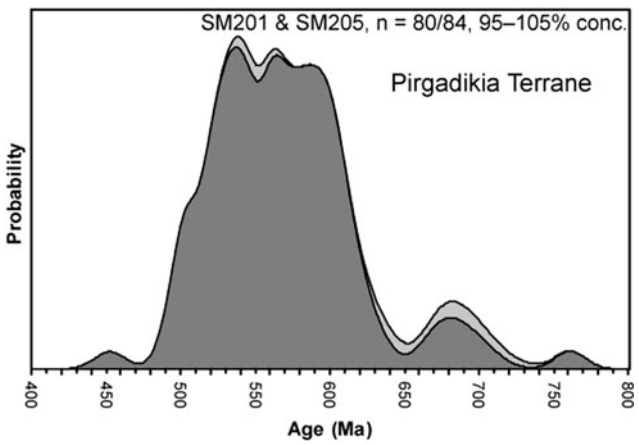

Fig. 9 Probability density distribution plot for the set of U–Pb analytical zircon data from samples SM201 and SM205 of the Pirgadikia Terrane for the time range between 400 and 800 Ma. Probability density distribution plots: *Dark grey* shaded zircon ages with 95–105% concordance, *light grey* shaded zircon ages with >5% discordance (see text for explanation). *n* Number of analyses

almost absent in sample SM205. The concordance-filtered zircon ages of 60 analyses on 59 single grains from sample SM201 show a polymodal age distribution with major peaks at ca. 530, 590 and 690 Ma, a subordinate cluster at ca. 950–1,200, and a scatter of ages between ca. 1,370 and 2,820 Ma (Fig. 8a, c). The youngest nearly concordant grain is 501 ± 18 Ma old and belongs to a group of four detrital zircons with a rounded shape and $^{206}Pb/^{238}U$ ages ranging between 501 ± 18 and 509 ± 17 Ma. The presence of Mesoproterozoic (~1,000 Ma), Palaeoproterozoic (1,800–2,200 Ma) and Archaean (~2,500 Ma) sources is also demonstrated by discordant grains that probably suffered radiogenic lead loss. The oldest grain has a $^{207}Pb/^{206}Pb$ age of 2,821 ± 22 Ma.

The concordance-filtered zircon ages of 48 analyses on 42 single grains from sample SM205 show a similar pattern to that of sample SM201, with a polymodal age distribution between 500 and 700 Ma but a virtual absence of older ages, with only three minor peaks at ca. 760, 1,350 and

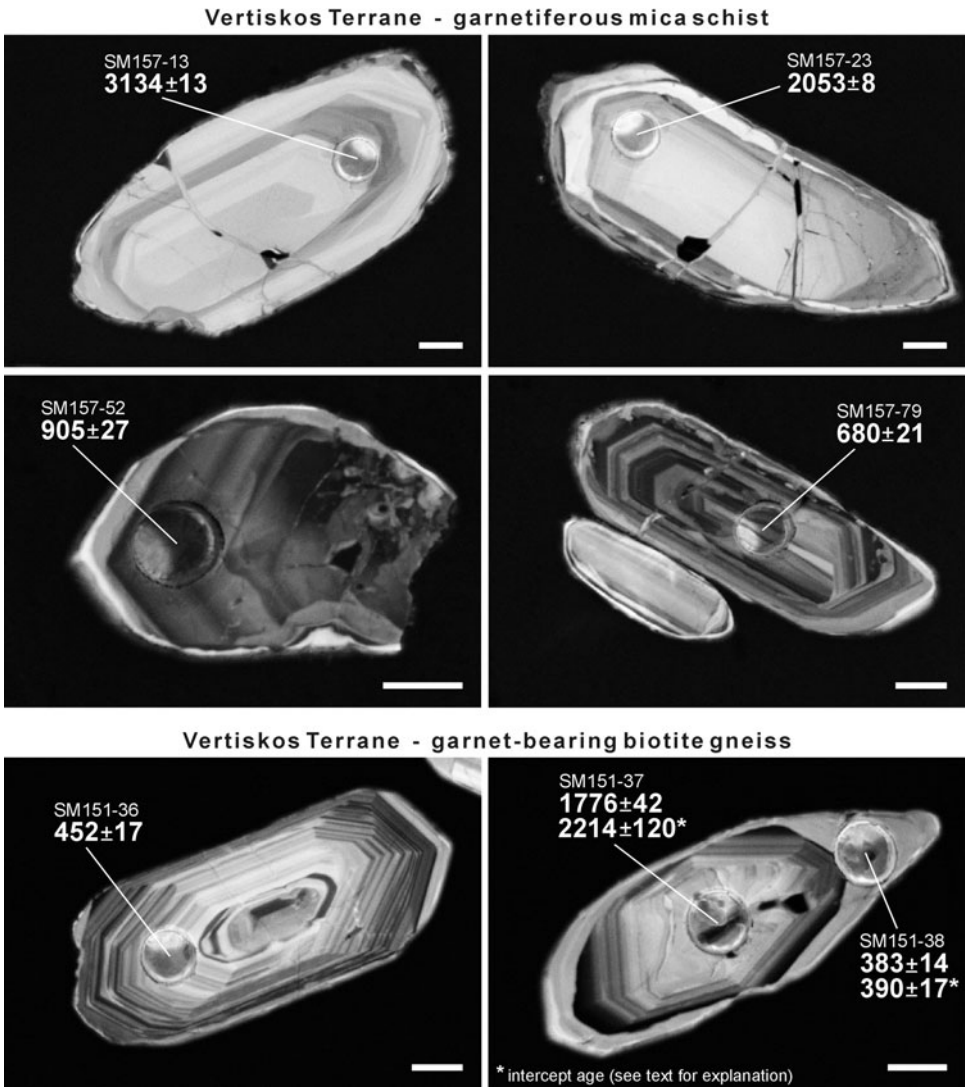

Fig. 10 CL images of representative zircon grains from analysed samples SM157 and SM151 of the Vertiskos Terrane with location of the LA-SF-ICP-MS analysis spot and corresponding $^{206}U/^{238}Pb$ age ($\pm 2\sigma$) for grains <1.2 Ga and $^{207}Pb/^{206}Pb$ age ($\pm 2\sigma$) for grains >1.2 Ga, respectively. *Letter*, *number* code above the ages: sample-spot. The *scale bar* represents 30 μm in all images

1,500 Ma (Fig. 8b, d). Major peaks occur at ca. 500 Ma and 565 Ma; a less prominent peak appears at ca. 675 Ma. The youngest nearly concordant grain is well rounded and has a $^{206}Pb/^{238}U$ age of 453 ± 22 Ma. The youngest group of zircons includes three concordant grains with $^{206}Pb/^{238}U$ ages of 492 ± 17, 499 ± 15 and 502 ± 13 Ma. The oldest concordant grain has a $^{207}Pb/^{206}Pb$ age of 1519 ± 23 Ma.

The analyses of both samples from the Pirgadikia Terrane are combined in Fig. 9, which focuses on the age spectrum between 400 and 800 Ma. Two major periods, at ca. 490–630 Ma and 660–710 Ma, can be identified which may represent distinct periods of zircon growth in Neoproterozoic and Cambrian times.

Vertiskos Terrane

Most zircons analysed from garnetiferous mica schist SM157 have clear oscillatory zonation patterns in CL images and appear to be magmatic in origin (Fig. 10); only a few exhibit no zoning. Inherited cores are present to a minor degree. The concordance-filtered zircon ages of 60 single-grain analyses show a predominance of zircons in the 550–1,050 Ma range with major peaks at ca. 570, 620, 670 and 770 Ma, and a cluster at ca. 900–1,050 Ma. The two youngest grains in sample SM157 are rounded and have $^{206}Pb/^{238}U$ ages of 459 ± 20 and 493 ± 17 Ma, respectively. The first of the two grains, however, has a Th/U value <0.1 and its age cannot therefore be considered as magmatic; it rather suggests post-depositional metamorphic re-crystallisation. The gap that exists in ages between 1,100 and 1,760 Ma should also be noted. A second zircon population shows Palaeoproterozoic and Archaean ages with single peaks at ca. 1,760, 1,950, 2,050, 2,080, 2,430 and 3,130 Ma (Fig. 11a, c). These peaks, however, are based on a very limited number of analyses only and stand out because of the relatively small errors in their $^{207}Pb/^{206}Pb$ ratios. The presence of Palaeoproterozoic (~2,000 Ma) and Archaean (~2,600 Ma) sources is also

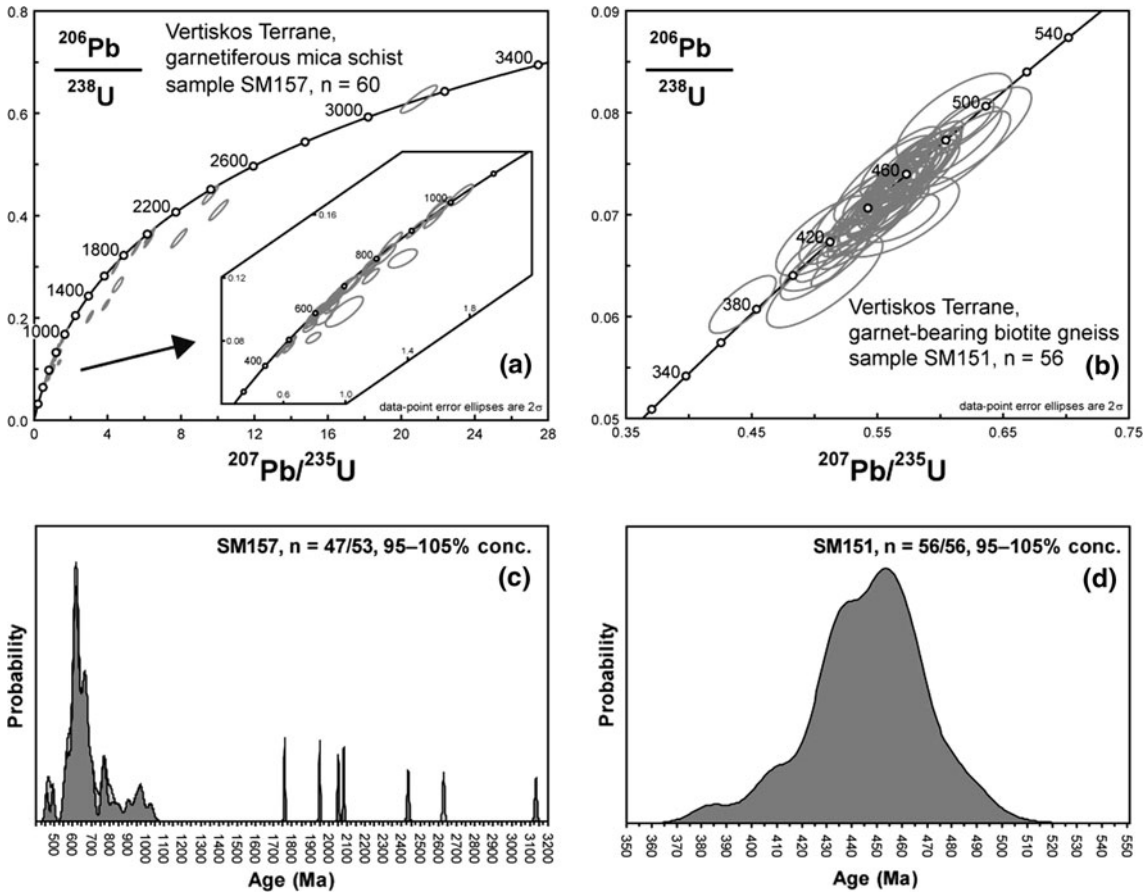

Fig. 11 Concordia diagrams (*upper*) and combined probability density distribution plots (*lower*) for the set of U–Pb analytical zircon data from sample SM157 (**a**, **c**) and SM151 (**b**, **d**). Two highly discordant grains of sample SM151 with $^{207}Pb/^{206}Pb$ ages of 1776 ± 21 Ma (1σ) and 2715 ± 8 Ma (1σ), respectively, are not shown. Error ellipses in concordia plots represent 2σ uncertainties. 1.2 Ga limit is used to switch between $^{206}Pb/^{238}U$ and $^{207}Pb/^{206}Pb$ ages for the probability plot. Probability density distribution plots: *dark grey* shaded zircon ages with 95–105% concordance, *light grey* shaded zircon ages with >5 % discordance (see text for explanation). *n* Number of analyses

demonstrated by discordant grains (see also Fig. 11a, c) that probably suffered radiogenic lead loss. The oldest concordant grain has a $^{207}Pb/^{206}Pb$ age of 3,134 ± 13 Ma.

Zircons from garnet-bearing biotite gneiss SM151 are very homogeneous. They display clear oscillatory zonation patterns in CL images and appear to be magmatic in origin. Inherited cores are almost absent. The concordance-filtered zircon ages of 58 single-grain analyses show an age distribution between ca. 400 and 500 Ma, with major peaks at ca. 435 and 455 Ma (Fig. 11b, d). The presence of Palaeoproterozoic (ca. 1.8 Ga) and Late Archaean (ca. 2.7 Ga) sources may be documented by two highly discordant zircon grains (see Table 4 of supplementary material) that probably suffered radiogenic lead loss. One analysis of a zircon overgrowth yielded a slightly reverse discordant $^{206}Pb/^{238}U$ age of 383 ± 14 Ma which is the youngest age determined in this sample. The oldest concordant grain in sample SM151 has a $^{206}Pb/^{238}U$ age of 493 ± 22 Ma.

Discussion and conclusions

Pirgadikia Terrane

Petrology and geochemistry indicate that the metasedimentary rocks of the Pirgadikia Terrane are characterised by very mature sandstones, siltstones and minor conglomerates, mainly composed of weathering-resistant quartz clasts. Detrital zircon age spectra from samples SM201 and SM205 differ slightly but both show a prominent age cluster between 490 and 710 Ma that indicates denudation of Pan-African basement. Deposition in proximity to Pan-African basement was already suggested by Himmerkus et al. (2006a) based on single-zircon Pb–Pb ages from one metaquartzite sample near Taxiarchis village. As shown here the interval between 490 and 710 Ma comprises two major events, at ca. 490–630 and 660–710 Ma, with the former one comprising several events.

Interestingly, a similar spectrum was obtained by Gerdes and Zeh (2006) for a high-grade metasediment from the Mid-German Crystalline Rise that was interpreted as indicating distinct periods of magma formation during the Neoproterozoic to Cambrian, at ca. 500–515, 545, 575–595 and 640–720 Ma. Following Gerdes and Zeh (2006), the 670–710 and 560–620 Ma-old zircons from the Pirgadikia Terrane might have formed in an island-arc or continental-arc setting related to the formation of the Avalonian–Cadomian orogenic belt, whereas zircons at ca. 520–550 Ma were most probably formed during late-orogenic magmatism related to the Cadomian orogeny. Zircons ca. 490–510 Ma old can be related to rifting processes and back-arc opening of the Rheic Ocean, separating Avalonian and later on Armorican terranes from the northern margin of Gondwana (e.g. von Raumer et al. 2002, 2003, and references therein).

Here, it is worth mentioning that the zircon age spectrum of the Pirgadikia samples carries an interesting parallel with the exposed Avalonian basement in England and Wales, which have the largest preserved Avalonian inliers in Western Europe (e.g. Winchester et al. 2006, and references therein). In these areas, the Uriconian volcanism peaked around 560 Ma (e.g. Strachan et al. 1996), with earlier dates have also been obtained corresponding to the earlier peak referred to in this study. Notable are 677 ± 2 Ma for the Malvern intrusion in central England (Strachan et al. 1996), and a 666 ± 7 Ma age for the metamorphism of the Coedana gneisses on Anglesey (Strachan et al. 2007).

The maximum depositional age of the metasedimentary rocks from the Pirgadikia Terrane can be constrained by the youngest detrital zircons. Preliminary single-zircon Pb–Pb age determinations by Himmerkus et al. (2006a) gave an age of ca. 530 Ma as youngest detrital input. In the present study, however, much younger ages have been found: 501 ± 18 Ma for sample SM201 and 453 ± 22 Ma for sample SM205. The former age seems geologically meaningful since it belongs to a group of ages that cluster between ca. 501 and 509 Ma. The latter, however, is a single age determination and should therefore be interpreted with care. The youngest age group in sample SM205 comprises zircons between ca. 492 and 502 Ma. The roundness of the zircon grains suggests prolonged reworking, due to either long-distance transport by river systems or long-lasting abrasion in a coastal environment. Keeping in mind both the geological frame and time necessary for uplift and erosion of plutonic rocks and that necessary for weathering, transport and abrasion, we propose that the sedimentary rocks of the Pirgadikia Terrane are younger than Cambrian, probably Early-Middle Ordovician, whereas an even younger age cannot be excluded insofar as no biostratigraphic or other geochronological data are available. However, a correlation with Upper Palaeozoic–Lower Mesozoic rocks from the Aegean region, as speculated by Himmerkus et al. (2006a: 45), based on $^{87}Sr/^{86}Sr$ initial ratios, seems most unlikely since these rocks contain also detrital zircons of Devonian and Carboniferous ages (Meinhold and Frei 2008; Meinhold et al. 2008).

The upper time limit for deposition is set by the structural and upper greenschist-facies metamorphic overprint that took place probably in the latest Jurassic–early Cretaceous. Nevertheless, an Ordovician age seems quite reasonable since, on a regional scale, the sedimentary rocks of the Pirgadikia Terrane share many similarities with those of the widespread Ordovician Armorican Quartzite Formation (Grès Armorican Formation and its equivalents), a succession of continental or marine, very mature quartzitic sandstones sometimes associated with conglomerates and arkosic sandstones (e.g. Noblet and Lefort 1990). In many parts of North Africa and Europe the Armorican Quartzite Formation conformably or unconformably overlies the Pan-African basement or Cambrian sedimentary rocks (e.g. Noblet and Lefort 1990). Its deposition was constrained by a lower-intercept age of ca. 465 Ma on zircons from an intercalated rhyolitic tuff (Bonjour et al. 1988) and provides a minimum age for the amalgamation of West Africa- and Amazonia-derived terranes by strike-slip motion along the northern margin of Gondwana that resulted in the Armorican Terrane Collage (Fernández-Suárez et al. 2002). The formation of very mature quartzose sediments of Cambrian–Ordovician age along the entire northern margin of Gondwana (Noblet and Lefort 1990; Avigad et al. 2005) is not yet fully understood. Linnemann and Romer (2002) suggest increased reworking of older sediments that formed during various hiatus of sedimentation. In comparison, Avigad et al. (2005) suggest they are essentially first-cycle sediments and reflect intense chemical weathering processes, particularly in a warm and humid climate, accompanied by low relief and low sedimentation rates. This led to the destruction of unstable fragments during erosion and weathering of the source rocks and thus increased the sediment maturity before final deposition.

Besides zircon grains that range in age between 490 and 710 Ma, Mesoproterozoic, Palaeoproterozoic and Late Archaean zircons are also present although in minor amounts. The older ones ($\geq$1.6 Ga) probably represent recycled zircons rather than zircons that have been directly derived from Palaeoproterozoic or Late Archaean rocks. Zircons of such ages match the spread of orogenic events recorded in the West African and eastern Amazonian cratons (e.g. Nance and Murphy 1994, 1996). Palaeoproterozoic (ca. 1.8–2.1 Ga) basement is also known from Brittany and the Channel Islands in Western Europe (Calvez and Vidal 1978; Samson and D'Lemos 1998).

The Mesoproterozoic concordant zircon grains are of palaeotectonic significance, especially those with ages around 1.5 Ga (Gothian–Rondonian–Rio Negro events) in combination with grains around 1.0 Ga old (Sveconorwegian–Grenvillian events). Similar ages were reported from NW Iberia (Fernández-Suárez et al. 2002), the NE Bohemian Massif (Hegner and Kröner 2000; Mingram et al. 2004), the Moravo–Silesian Unit (Friedl et al. 2000, 2004), West Avalonia (Nance and Murphy 1994, 1996), East Avalonia (Strachan et al. 2007), the Małopolska Unit (Belka et al. 2002) and the Polish East European Platform (Belka et al. 2002). Such ages, however, are not known from the Meguma Terrane (Nance and Murphy 1996), Saxothuringia (e.g. Linnemann et al. 2004), SW Iberia and Brittany (Fernández-Suárez et al. 2002), meaning that they are absent in rocks which have their source in the West African Craton. In north-western Greece, Anders et al. (2006) obtained $^{206}Pb/^{207}Pb$ ages ranging between ca. 800 and 1,340 Ma and a concordant $^{206}Pb/^{238}U$ SHRIMP-II age of 1,500 ± 18 Ma from inherited zircons in Neoproterozoic orthogneisses (ca. 700 Ma) from the Florina Terrane. The Florina Terrane constitutes the basement of the NW Pelagonian Zone and has affinities with East Avalonia (Anders et al. 2006). In general, inherited and detrital zircon ages of ca. 1 and 1.5 Ga are well known from Avalonia supporting a position adjacent to the Amazonian Craton at the end of the Neoproterozoic whereas Armorican terranes lack such a component, suggesting closer affinities with the West African Craton (Nance and Murphy 1996; Samson et al. 2005; Winchester et al. 2006).

In the Eastern Mediterranean, the closest localities with quartz-rich sediments similar to those of the Pirgadikia Terrane can be found in the Istanbul and Zonguldak Terranes of northern Turkey (see Yanev et al. 2006). In the latter terrane, for instance, pre-Cambrian basement rocks are unconformably overlain by Lower Ordovician sandstones and conglomerates (Dean et al. 2000). Ordovician trilobite fauna from the Zonguldak Terrane indicate a close relation to Ordovician successions from central Europe (Bohemia) and the Anglo-Welsh Basin (Avalonia) (Dean et al. 2000). The Zonguldak Terrane may have been located along the eastern continuation of Avalonia and the Moravo-Silesian Terrane (Yanev et al. 2006). Ordovician and Silurian benthic fauna from the Istanbul Terrane are of Avalonian and Podolian affinity, whereas Devonian brachiopods and trilobites are clearly of Bohemian and North African affinity (Yanev et al. 2006). The Balkan and NW Anatolian Terranes were part of northern Gondwana but not of Baltica (Yanev et al. 2006, and references therein).

To conclude, the Pirgadikia Terrane comprises island-arc basement (ca. 570–580 Ma: Himmerkus et al. 2006a, 2007) of the Avalonian–Cadomian orogenic belt and very mature quartzose sediments of probably Early–Middle Ordovician age (this study). Detrital zircon ages reflect derivation of these sediments from at least three distinct crustal sources, i.e. the Avalonian–Cadomian belt, the West African and/or Amazonian cratons and the Grenvillian belt, which may be taken as evidence for an Avalonian origin of the Pirgadikia Terrane. The 490–510 Ma-old detrital zircons can be related to Upper Cambrian igneous rocks probably emplaced in a transtensional setting. Thus, in the Late Neoproterozoic–Early Palaeozoic, the Pirgadikia Terrane can be best interpreted as a peri-Gondwana terrane, situated in the Avalonian realm north of the evolving Rheic Ocean but in proximity to Cadomian terranes (Fig. 12), very much like the "Avalonian satellites" of von Raumer et al. (2003). The history of the Pirgadikia Terrane throughout the Palaeozoic and Mesozoic, however, is still enigmatic because of the lack of palaeogeographic constraints (e.g. palaeomagnetic data and fauna) for that time. Today, the rocks of the Pirgadikia Terrane occur in isolated fault-bounded inliers within the Vardar zone bordering the Serbo-Macedonian Massif to the west.

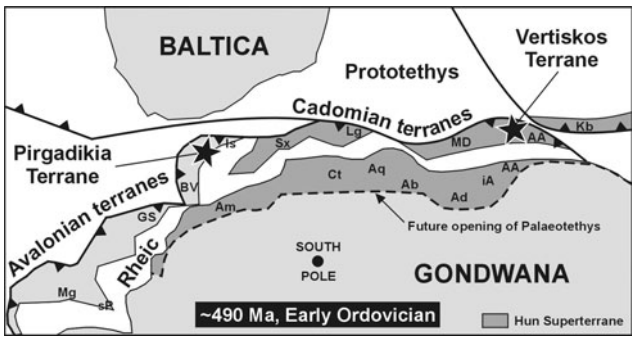

Fig. 12 Early Ordovician (~490 Ma) plate-tectonic reconstruction showing presumed location of the Pirgadikia and the Vertiskos Terranes (*black stars*) in the peri-Gondwana realm (modified from von Raumer et al. 2003). *AA* Austro-Alpine, *Ab* Alboran plate, *Ad* Adria sensu stricto, *Am* Armorica, *Aq* Aquitaine, *Ct* Cantabria, *iA* Intra-Alpine terrane, *GS* Gory Sowie, *Kb* Karaburun, *Mg* Meguma, *sP* South Portuguese, *BV* Bruno-Vistulikum, *Is* Istanbul terrane, *Lg* Ligeria, *MD* Moldanubia, *Sx* Saxothuringia

Vertiskos Terrane

The detrital zircon age spectrum from the garnetiferous mica schist shows a prominent age cluster between 550 and 800 Ma, indicating denudation of the Cadomian and Pan-African basement. The gap in zircon ages between 500 and 550 Ma suggests that there was no input of rocks from the source area related to late-orogenic tectonothermal events of the Cadomian orogeny. On the basis of the $^{206}Pb/^{238}U$ age of 493 ± 17 Ma, the maximum age of deposition is suggested to be Early Ordovician with an upper time limit for deposition given by the intrusion of the Upper

Ordovician–Silurian magmatic rocks into the metasedimentary succession.

The ca. 900–1050 Ma-old zircons are assumed to be derived from the Grenvillian orogenic belt and might have been transported by large river systems to the northern margin of Gondwana (Zeh et al. 2001). The few Palaeoproterozoic (>1.7 Ga) and Archaean zircons probably represent recycled zircons, rather than zircons directly derived from Palaeoproterozoic and Archaean rocks. Zircons of such ages match the spread of orogenic events recorded in the West African and eastern Amazonian cratons (e.g. Nance and Murphy 1994, 1996). Taking all data collectively, the Pan African (ca. 550–800), Grenvillian (900–1,050 Ma), Icartian–Eburnean (1,950–2,100 Ma) and minor Archaean (>2.5 Ga) ages, together with the gap in ages between 1,050 and 1,760 Ma found in the garnetiferous mica schist studied clearly indicate a North Gondwana signature. At this point we suggest that the sedimentary protolith of the garnetiferous mica schist, and on a larger scale, most of the metasedimentary rocks of the Vertiskos Terrane, were deposited in a Cadomian realm (future Hun superterrane), probably prior to the final breakoff from the northern margin of Gondwana (Fig. 12). Their palaeotectonic position within the Cadomian realm can be further constrained by analysis of the intrusive rocks.

The zircon ages from the garnet-bearing biotite gneiss cover a wide time span from ca. 405 to 490 Ma with major peaks around 435 and 455 Ma. They fit Ordovician and Silurian ages of acidic meta-magmatites from the Vertiskos Terrane (see Himmerkus et al. 2006a, 2007, 2008) and presumably those of equivalent rocks from SW Bulgaria (e.g. Titorenkova et al. 2003), and are interpreted here to be typical of the older part of the Serbo-Macedonian Massif. The extension of these basement rocks into western Turkey can also be anticipated since a $^{207}Pb/^{206}Pb$ single-zircon evaporation age of around 462 Ma was documented for orthogneisses from the Biga Peninsula in NW Turkey (Özmen and Reischmann 1999). Bright overgrowths of some zircons observed in CL images indicate reheating of the Vertiskos basement and new zircon growth during a late Early Devonian event (ca. 390 Ma). The age information, in conjunction with the geochemical signature of the orthogneisses (volcanic-arc granites showing within-plate affinities) suggest that Vertiskos Terrane most probably originated in the eastern Hun superterrane (Himmerkus et al. 2007, 2008; this study), as did the Austro- and Intra-Alpine Terranes (Fig. 12) where Ordovician and Silurian magmatic episodes are well documented and related to an active-margin setting (e.g. Neubauer 2002; von Raumer et al. 2002). The final breakoff of these terranes from the northern margin of Gondwana was accompanied by the opening of the Palaeotethys Ocean to the south.

Since Carboniferous magmatic and metamorphic events have not yet been reported from the Vertiskos Terrane we suggest the following possibility for the location of the Vertiskos Terrane at the northern margin of Gondwana and its evolution through time. The model centres on the affiliation of Vertiskos to units of the eastern Hun superterrane, which in our opinion best fits the data. The Vertiskos Terrane (along with Moldanubia and the Austro- and Intra-Alpine Terranes) rifted away from the northern margin of Gondwana, leading to the opening of the Palaeotethys Ocean to the south. Later, it was "softly" accreted by transcurrent movements in the Devonian–Carboniferous to the southern margin of Laurussia, whence it rifted in the Early–Middle Triassic (intrusion of the within-plate Arnea granitic suite) and was again involved in subduction-accretion processes during the Late Jurassic to Early Cretaceous, when a branch of the Vardar Ocean closed.

Acknowledgments This study was supported by the German Research Foundation and the state of Rhineland–Palatinate through the Graduiertenkolleg 392 "Composition and Evolution of Crust and Mantle". Laboratory facilities at the Max-Planck-Institute for Chemistry, at the Institute of Geosciences in Mainz and at the Geological Survey of Denmark and Greenland in Copenhagen are gratefully acknowledged. We thank Prof. John A. Winchester for his constructive review. This paper is published with the permission of the Geological Survey of Denmark and Greenland.

References

Aleksić V, Dimitriadis S, Kalenić M, Stojanov R, Zagorčev I (1988) Precambrian in the Serbo-Macedonian Massif. In: Zoubek V, Cogné J, Kozhoukharov D, Kräutner HG (eds) Precambrian in younger fold belts; Europe and Variscides, the Carpathians and Balkans. Wiley, New York, pp 779–820

Anders B, Reischmann T, Kostopoulos D, Poller U (2006) The oldest rocks of Greece: first evidence for a Precambrian terrane within the Pelagonian Zone. Geol Mag 143:41–58. doi:10.1017/S0016756805001111

Avigad D, Sandler A, Kolodner K, Stern RJ, McWilliams M, Miller N, Beyth M (2005) Mass-production of Cambro-Ordovician quartz-rich sandstones as a consequence of chemical weathering of Pan-African terranes: environmental implications. Earth Planet Sci Lett 240:818–826. doi:10.1016/j.epsl.2005.09.021

Belka Z, Valverde-Vaquero P, Dörr W, Ahrendt H, Wemmer K, Franke W, Schäfer J (2002) Accretion of first Gondwana-derived terranes at the margin of Baltica. In: Winchester JA, Pharaoh TC, Verniers J (eds) Palaeozoic Amalgamation of Central Europe, vol 201. Geol Soc Lond Spec Publ, pp 19–36

Bonjour JL, Peucat JJ, Chauvel JJ, Paris F, Cornichet J (1988) U-Pb zircon dating of the Early Paleozoic (Arenigian) transgression in

western Brittany (France): a new constraint for the Lower Paleozoic time-scale. Chem Geol 72:329–336
Brun JP, Sokoutis D (2007) Kinematics of the Southern Rhodope Core Complex (North Greece). Int J Earth Sci 96:1079–1099. doi:10.1007/s00531-007-0174-2
Burg JP, Godfriaux I, Ricou LE (1995) Extension of the Mesozoic Rhodope thrust units in the Vertiskos-Kerdilion Massifs (Northern Greece). C R Acad Sci Paris 320:889–896
Burg JP, Ricou LE, Ivanov Z, Godfriaux I, Dimov D, Klain L (1996) Syn-metamorphic nappe complex in the Rhodope Massif. Structure and kinematics. Terra Nova 8:6–15. doi:10.1111/j.1365-3121.1996.tb00720.x
Calvez JY, Vidal P (1978) Two billion year old relicts in the Hercynian belt of western Europe. Contrib Mineral Petrol 65:395–399. doi:10.1007/BF00372286
Dean WT, Monod O, Rickards RB, Demir O, Bultynck P (2000) Lower Palaeozoic stratigraphy and palaeontology, Karadere-Zirze area, Pontus Mountains, northern Turkey. Geol Mag 137:555–582. doi:10.1017/S0016756800004635
Dinter DA, Royden L (1993) Late Cenozoic extension in the northeastern Greece: Strimon Valley detachment system and Rhodope metamorphic core complex. Geology 21:45–48. doi:10.1130/0091-7613(1993)021<0045:LCEING>2.3.CO;2
Dixon JE, Dimitriadis S (1984) Metamorphosed ophiolitic rocks from the Serbo-Macedonian Massif near Lake Volvi, north-east Greece. In: Dixon JE, Robertson AHF (eds) The geological evolution of the eastern Mediterranean, vol 17. Geol Soc Lond Spec Publ, pp 603–618
Fedo CM, Sircombe KN, Rainbird RH (2003) Detrital zircon analysis of the sedimentary record, vol 53. In: Hanchar JM, Hoskin PO (eds) Zircon, vol 53. Rev Mineral Geochem, pp 277–303
Fernández-Suárez J, Gutiérrez Alonso G, Jeffries TE (2002) The importance of along-margin terrane transport in northern Gondwana: insights from detrital zircon parentage in Neoproterozoic rocks from Iberia and Brittany. Earth Planet Sci Lett 204:75–88. doi:10.1016/S0012-821X(02)00963-9
Frei D, Gerdes A (2008) Precise and accurate in situ U–Pb dating of zircon with high sample throughput by automated LA-SF-ICP-MS. Chem Geol. doi:10.1016/j.chemgeo.2008.07.025
Friedl G, Finger F, McNaughton NJ, Fletcher IR (2000) Deducing the ancestry of terranes: SHRIMP evidence for South America-derived Gondwana fragments in central Europe. Geology 28:1035–1038. doi:10.1130/0091-7613(2000)28<1035:DTAOTS>2.0.CO;2
Friedl G, Finger F, Paquette J-L, von Quadt A, McNaughton NJ, Fletcher IR (2004) Pre-Variscan geological events in the Austrian part of the Bohemian Massif deduced from U–Pb zircon ages. Int J Earth Sci 93:802–823. doi:10.1007/s00531-004-0420-9
Gerdes A, Zeh A (2006) Combined U–Pb and Hf isotope LA-(MC)-ICP-MS analyses of detrital zircons: comparison with SHRIMP and new constraints for the provenance and age of an Armorican metasediment in Central Germany. Earth Planet Sci Lett 249:47–61. doi:10.1016/j.epsl.2006.06.039
Gradstein FM, Ogg JG, Smith AG (2004) A geologic time scale 2004. Cambridge University Press, Cambridge, pp 1–610
Hegner E, Kröner A (2000) Review of Nd isotopic data and xenocrystic and detrital zircon ages from the pre-Variscan basement in the eastern Bohemian Massif: speculations on palinspastic reconstructions. In: Franke W, Haak V, Oncken O, Tanner D (eds) Orogenic processes: quantification and modelling in the Variscan Belt, vol 179. Geol Soc Lond Spec Publ, pp 113–129
Herron MM (1988) Geochemical classification of terrigenous sands and shales from core or log data. J Sed Petrol 58:820–829
Himmerkus F, Reischmann T, Kostopoulos D (2006a) Late Proterozoic and Silurian basement units within the Serbo-Macedonian Massif, northern Greece: the significance of terrane accretion in the Hellenides. In: Robertson AHF, Mountrakis D (eds) Tectonic development of the Eastern Mediterranean Region, vol 260. Geol Soc Lond Spec Publ, pp 35–50
Himmerkus F, Reischmann T, Kostopoulos D (2006b) Permo-Carboniferous and upper Jurassic basement ages in the Kerdillion Unit, eastern Serbo-Macedonian Massif, northern Greece. Geophys Res Abstr 8:05758
Himmerkus F, Anders B, Reischmann T, Kostopoulos D (2007) Gondwana-derived terranes in the northern Hellenides. In: Hatcher RD Jr, Carlson MP, McBride JH, Martínez Catalán JR (eds) 4-D Framework of continental crust, vol 200. Geol Soc Am Mem, pp 379–390
Himmerkus F, Reischmann T, Kostopoulos D (2008) Serbo-Macedonian revisited: a Silurian basement terrane from northern Gondwana in the Internal Hellenides, Greece. Tectonophysics. doi:10.1016/j.tecto.2008.10.016
Himmerkus F, Reischmann T, Kostopoulos D (2009) Triassic rift-related meta-granites in the Internal Hellenides, Greece. Geol Mag 146:252–265. doi:10.1017/S001675680800592X
Horstwood MSA, Foster GL, Parrish RR, Noble SR, Nowell GM (2003) Common-Pb corrected in situ U–Pb accessory mineral geochronology by LA-MC-ICP-MS. J Anal At Spectrom 18:837–846. doi:10.1039/b304365g
Jackson S, Pearson NJ, Griffin WL, Belousova EA (2004) The application of laser ablation-inductively coupled plasma-mass spectrometry to in situ U–Pb zircon geochronology. Chem Geol 211:47–69. doi:10.1016/j.chemgeo.2004.06.017
Jacobshagen V (1986) Geologie von Griechenland. Gebrüder Borntraeger, Berlin, pp 1–363
Janoušek V, Gerdes A, Vrána S, Finger F, Erban V, Friedl G, Braithwaite CJR (2006) Low-pressure Granulites of the Lišov Massif, Southern Bohemia: Viséan Metamorphism of Late Devonian Plutonic Arc Rocks. J Petrol 47:705–744. doi:10.1093/petrology/egi091
Kilias A, Falalakis G, Mountrakis D (1999) Cretaceous–Tertiary structures and kinematics of the Serbomacedonian metamorphic rocks and their relation to the exhumation of the Hellenic hinterland (Macedonia, Greece). Int J Earth Sci 88:513–531. doi:10.1007/s005310050282
Kockel F, Walther HW (1965) Die Strimonlinie als Grenze zwischen Serbo-Mazedonischen und Rila-Rhodope-Massif in Ost-Mazedonien. Geol J 83:575–602
Kockel F, Mollat H (1977) Geological map of the Chalkidiki peninsula and adjacent areas (Greece), scale 1:100,000. Bundesanst Geowiss Rohstoffe, Hannover
Kockel F, Mollat H, Walther HW (1971) Geologie des Serbo-Mazedonischen Massivs und seines mesozoischen Rahmens (Nordgriechenland). Geol Jahrb 89:529–551
Kockel F, Mollat H, Walther HW (1977) Erläuterungen zur Geologischen Karte der Chalkidiki und angrenzender Gebiete 1:100,000 (Nord-Griechenland). Bundesanst Geowiss Rohstoffe, Hannover, pp 1–119
Košler J, Fonneland H, Sylvester P, Tubrett M, Pedersen RB (2002) U–Pb dating of detrital zircons for sediment provenance studies—a comparison of laser ablation ICPMS and SIMS techniques. Chem Geol 182:605–618. doi:10.1016/S0009-2541(01)00341-2
Linnemann U, Romer RL (2002) The Cadomian Orogeny in Saxo-Thuringia, Germany: geochemical and Nd-Sr-Pb isotopic characterization of marginal basins with constraints to geotectonic setting and provenance. Tectonophysics 352:33–64. doi:10.1016/S0040-1951(02)00188-9
Linnemann U, McNaughton NJ, Romer RL, Gehmlich M, Drost K, Tonk C (2004) West African provenance for Saxo-Thuringia (Bohemian Massif): did Armorica ever leave pre-Pangean

Gondwana?—U/Pb-SHRIMP zircon evidence and the Nd-isotopic record. Int J Earth Sci 93:683–705. doi:10.1007/s00531-004-0413-8

Ludwig KR (2003) Isoplot/Ex 3.00. A Geochronological Toolkit for Microsoft Excel. Berkeley Geochron Cent Spec Publ 4:1–70

IGME (1983) Geological map of Greece, scale 1:500,000. Institute of Geology and Mineral Exploration, Athens

Meinhold G, Frei D (2008) Detrital zircon ages from the islands of Inousses and Psara, Aegean Sea, Greece: constraints on depositional age and provenance. Geol Mag 145:886–891. doi:10.1017/S0016756808005505

Meinhold G, Kostopoulos D, Reischmann T (2007) Geochemical constraints on the provenance and depositional setting of sedimentary rocks from the islands of Chios, Inousses and Psara, Aegean Sea, Greece: implications for the evolution of Palaeotethys. J Geol Soc London 164:1145–1163. doi:10.1144/0016-76492006-111

Meinhold G, Reischmann T, Kostopoulos D, Lehnert O, Matukov D, Sergeev S (2008) Provenance of sediments during subduction of Palaeotethys: detrital zircon ages and olistolith analysis in Palaeozoic sediments from Chios Island, Greece. Palaeogeogr Palaeoclimatol Palaeoecol 263:71–91. doi:10.1016/j.palaeo.2008.02.013

Mezger K, Krogstad EJ (1997) Interpretation of discordant U–Pb zircon ages: an evaluation. J Metamorph Geol 15:127–140. doi:10.1111/j.1525-1314.1997.00008.x

Mingram B, Kröner A, Hegner E, Krentz O (2004) Zircon ages, geochemistry, and Nd isotopic systematics of pre-Variscan orthogneisses from the Erzgebirge, Saxony (Germany), and geodynamic interpretation. Int J Earth Sci 93:706–727. doi:10.1007/s00531-004-0414-7

Murphy JB, Fernández-Suárez J, Keppie JD, Jeffries TE (2004) Continuous rather than discrete Paleozoic histories for the Avalon and Meguma terranes based on detrital zircon data. Geology 32:585–588. doi:10.1130/G20351.1

Nance RD, Murphy JB (1994) Contrasting basement isotopic signatures and the palinspastic restoration of peripheral orogens; example from the Neoproterozoic Avalonian-Cadomian belt. Geology 22:617–620. doi:10.1130/0091-7613(1994)022<0617:CBISAT>2.3.CO;2

Nance RD, Murphy JB (1996) Basement isotopic signatures and Neoproterozoic paleogeography of Avalonian-Cadomian and related terranes in the circum-North Atlantic. In: Nance RD, Thompson MD (eds) Avalonian and related peri-Gondwana terranes of the circum-North Atlantic, vol 304. Geol Soc Am Spec Pap, pp 333–345

Nehring F, Jacob DE, Barth MG, Foley SF (2008) Laser-ablation ICP-MS analysis of siliceous rock glasses fused on an Iridium strip heater using MgO dilution. Mikrochim Acta 160:153–163. doi:10.1007/s00604-007-0819-7

Neubauer F (2002) Evolution of late Neoproterozoic to early Paleozoic tectonic elements in Central and Southeast European Alpine mountain belts: review and synthesis. Tectonophysics 352:87–103. doi:10.1016/S0040-1951(02)00190-7

Noblet C, Lefort JP (1990) Sedimentological evidence for a limited separation between Armorica and Gondwana during the Early Ordovician. Geology 18:303–306. doi:10.1130/0091-7613(1990)018<0303:SEFALS>2.3.CO;2

Özmen F, Reischmann T (1999) The age of the Sakarya continent in W Anatolia: implications for the evolution of the Aegean region. J Conf Abstr 4:805

Passchier CW, Trouw RAJ (2005) Microtectonics, 2nd edn. Springer, Berlin, pp 1–366

Pearce JA, Harris NBW, Tindle AG (1984) Trace element discrimination diagrams for the tectonic interpretation of granitic rocks. J Petrol 25:956–983

Ricou L-E, Burg JP, Godfriaux I, Ivanov Z (1998) Rhodope and Vardar: the metamorphic and olistostromic paired belts related to the Cretaceous subduction under Europe. Geodin Acta 11:285–309. doi:10.1016/S0985-3111(99)80018-7

Rudnick RL, Gao S (2003) Composition of the continental crust. In: Holland HD, Turekian KK (eds) Treatise on geochemistry. Elsevier-Pergamon, Oxford, pp 1–64

Samson SD, D'Lemos RS (1998) U–Pb geochronology and Sm–Nd isotopic composition of Proterozoic gneisses, Channel Island, UK. J Geol Soc London 155:609–618. doi:10.1144/gsjgs.155.4.0609

Samson SD, D'Lemos RS, Miller BV, Hamilton MA (2005) Neoproterozoic palaeogeography of the Cadomian and Avalon terranes: constraints from detrital zircon U–Pb ages. J Geol Soc London 162:65–71. doi:10.1144/0016-764904-003

Şengör AMC, Yilmaz Y, Sungurlu O (1984) Tectonics of the Mediterranean Cimmerides: Nature and evolution of the western termination of Paleo-Tethys. In: Dixon JE, Robertson AHF (eds) The geological evolution of the eastern Mediterranean, vol 17. Geol Soc Lond Spec Publ, pp 77–112

Sircombe KN (2004) AgeDisplay: an EXCEL workbook to evaluate and display univariate geochronological data using binned frequency histograms and probability density distributions. Comput Geosci 30:21–31. doi:10.1016/j.cageo.2003.09.006

Sláma J, Košler J, Condon DJ, Crowley JL, Gerdes A, Hanchar JM, Horstwood MSA, Morris GA, Nasdala L, Norberg N, Schaltegger U, Schoene B, Tubrett MN, Whitehouse MJ (2008) Plešovice zircon—a new natural reference material for U–Pb and Hf isotopic microanalysis. Chem Geol 249:1–35. doi:10.1016/j.chemgeo.2007.11.005

Sokoutis D, Brun JP, Van Den Driessche J, Pavlides S (1993) A major Oligo-Miocene detachment in southern Rhodope controlling north Aegean extension. J Geol Soc London 150:243–246. doi:10.1144/gsjgs.150.2.0243

Stampfli GM, Borel GD (2002) A plate tectonic model for the Paleozoic and Mesozoic constrained by dynamic plate boundaries and restored synthetic oceanic isochrones. Earth Planet Sci Lett 196:17–33. doi:10.1016/S0012-821X(01)00588-X

Stampfli GM, von Raumer J, Borel GD (2002) Palaeozoic evolution of pre-Variscan terranes: From Gondwana to the Variscan collision. In: Martínez-Catalán JR, Hatcher RD, Arenas R, Díaz García F (eds) Variscan-Appalachian dynamics: the building of the late Paleozoic basement, vol 364. Geol Soc Am Spec Pap, pp 263–280

Strachan RA, Nance RD, Dallmeyer RD, D'Lemos RS, Murphy JB, Watt GR (1996) Late Precambrian tectonothermal evolution of the Malverns Complex. J Geol Soc London 153:589–600. doi:10.1144/gsjgs.153.4.0589

Strachan RA, Collins AS, Buchan C, Nance RD, Murphy JB, D'Lemos RS (2007) Terrane analysis along a Neoproterozoic active margin of Gondwana: insights from U–Pb zircon geochronology. J Geol Soc London 164:57–60. doi:10.1144/0016-76492006-014

Taylor SR, McLennan SM (1985) The continental crust: its composition and evolution. Blackwell, Oxford, pp 1–312

Titorenkova R, Macheva L, Zidarov N, von Quadt A, Peytcheva I (2003) Metagranites from SW Bulgaria as a part of the Neoproterozoic to early Paleozoic system in Europe: new insight from zircon typology, U–Pb isotope data and Hf-tracing. Geophys Res Abstr 5:08963

Turpaud P (2006) Characterisation of igneous terranes by zircon dating: implications for UHP relicts occurrences and suture identification in the Central Rhodope, Northern Greece. Ph.D. thesis, University of Mainz, Germany, pp 1–107

Turpaud P, Reischmann T (2005) Relationships between crustal blocks and UHP relics, an example from Northern Greece. Geophys Res Abstr 8:04353

von Raumer JF, Stampfli GM, Borel G, Bussy F (2002) Organization of pre-Variscan basement areas at the north-Gondwanan margin. Int J Earth Sci 91:35–52. doi:10.1007/s005310100200

von Raumer JF, Stampfli GM, Bussy F (2003) Gondwana-derived microcontinents—the constituents of the Variscan and Alpine collisional orogens. Tectonophysics 365:7–22. doi:10.1016/S0040-1951(03)00015-5

Williams IS (1992) Some observations on the use of zircon U–Pb geochronology in the study of granitic rocks. Trans R Soc Edinb Earth Sci 83:447–458

Winchester JA, Pharaoh TC, Verniers J, Ioane D, Seghedi A (2006) Palaeozoic accretion of Gondwana-derived terranes to the East European Craton: recognition of terrane fragments dispersed after collision with promontories. In: Gee D, Stephenson R (eds) European lithosphere dynamics, vol 32. Geol Soc Lond Mem, pp 323–332

Yanev S, Göncüoğlu MC, Gedik I, Lakova I, Boncheva I, Sachanski V, Okuyucu C, Özgül N, Timur E, Maliakov Y, Saydam G (2006) Stratigraphy, correlations and palaeogeography of Palaeozoic terranes of Bulgaria and NW Turkey: a review of recent data. In: Robertson AHF, Mountrakis D (eds) Tectonic development of the Eastern Mediterranean Region, vol 260. Geol Soc Lond Spec Publ, pp 51–67

Zeh A, Brätz H, Millar IL, Williams IS (2001) A combined zircon SHRIMP and Sm–Nd isotope study on high-grade paragneisses from the Mid-German Crystalline Rise: evidence for northern Gondwanan and Grenvillian provenance. J Geol Soc London 158:983–994. doi:10.1144/0016-764900-186